Published in final edited form as:
J Matern Fetal Neonatal Med. 2008 June ; 21(6): 367–388. doi:10.1080/14767050802045848.

Proteomic Analysis of Amniotic Fluid to Identify Women with Preterm Labor and Intra-amniotic Inflammation/Infection:

The Use of a Novel Computational Method to Analyze Mass Spectrometric Profiling

Roberto Romero, MD[1,2], **Jimmy Espinoza, MD**[1,3], **Wade T. Rogers, PhD**[4], **Allan Moser, PhD**[4], **Jyh Kae Nien, MD**[1], **Juan Pedro Kusanovic, MD**[1,3], **Francesca Gotsch, MD**[1], **Offer Erez, MD**[1,3], **Ricardo Gomez, MD**[5], **Sam Edwin, PhD**[1], and **Sonia S. Hassan, MD**[1,3]

1*Perinatology Research Branch, NICHD/NIH/DHHS, Bethesda, Maryland, and Detroit, Michigan, USA*

2*Center for Molecular Medicine and Genetics, Wayne State University, Detroit, Michigan, USA*

3*Department of Obstetrics and Gynecology, Wayne State University/Hutzel Hospital, Detroit, Michigan, USA*

4*Cira Discovery Sciences, Inc., Philadelphia, Pennsylvania, USA*

5*CEDIP, Department of Obstetrics and Gynecology, Sotero del Rio Hospital, Puente Alto, Chile*

Abstract

Objective—Examination of the amniotic fluid proteome has been used to identify biomarkers for intra-amniotic inflammation, as well as those that may be useful in predicting the outcome of preterm labor. The purpose of this study was to combine a novel computational method of pattern discovery with mass spectrometric proteomic profiling of amniotic fluid to discover biomarkers of intra-amniotic infection/inflammation (IAI).

Methods—This cross-sectional study included patients with spontaneous preterm labor and intact membranes who delivered at term (n=59) and those who delivered preterm with IAI (n=60). Proteomic profiling was performed using SELDI mass spectrometry. A proteomic profile was acquired through multiple simultaneous SELDI conditions which were combined in a single proteomic "fingerprint" using a novel computational approach. Classification of patients based on their associated SELDI-TOF mass spectra as belonging to either the class of individuals with preterm delivery with IAI or term delivery was accomplished by constructing an empirical model. The first phase in the construction of this empirical model involved the selection of adjustable parameters utilizing a training/testing subset of data. The second phase tested the generalization of the model by utilizing a blinded validation set of patients who were not employed in parameter selection.

Results—Gestational age at amniocentesis was not significantly different between the groups. Thirty-nine unique mass spectrometric peaks discriminated patients with preterm labor/delivery with IAI from those with preterm labor and term delivery. In the testing/training dataset, the classification accuracies (averaged over 100 random draws) were: 91.4% (40.2/44) for patients with preterm delivery with IAI, and 91.2% (40.1/44) for term delivery. The overall accuracy of the classification of patients in the validation dataset was 90.3% (28/31).

Conclusions—Proteomic analysis of amniotic fluid allowed the identification of mass spectrometry features which can distinguish patients with preterm labor with intra-amniotic infection/

Address correspondence to: Roberto Romero, MD Perinatology Research Branch, NICHD/NIH/DHHS Wayne State University/Hutzel Women's Hospital 3990 John R. — Box #4 Detroit, MI 48201 Phone: (313) 993-2700; Fax: (313) 993-2694 E-mail: prbchiefstaff@med.wayne.edu.

inflammation from those with preterm labor without inflammation or infection who subsequently delivered at term.

Keywords

Proteomics; preterm birth; intra-amniotic inflammation/infection; SELDI-TOF; mass spectrometry

Introduction

Preterm delivery is the leading cause of perinatal morbidity and mortality worldwide [1-4]. Two thirds of all preterm deliveries is the result of spontaneous preterm labor parturition approximately one third is the result of indicated delivery due to fetal and maternal indications [5,6]. The improved prognosis of preterm neonates is largely the consequence of advances in the care provided in newborn special care units [7], the availability of surfactant treatment [8-10], as well as the use of antenatal steroids [11,12]. The rate of spontaneous preterm birth remains largely unchanged and treatment with tocolysis has not been proven to reduce the rate of preterm delivery or perinatal morbidity and mortality [13-15]. Thus, the prevention of preterm delivery remains the most significant challenge of modern obstetrics.

Intrauterine infection is a common and important cause of spontaneous preterm labor and delivery. Standard microbiological techniques have demonstrated that at least 25% of all preterm births occur to mothers with microbial invasion of the amniotic cavity (MIAC) [16]. However, there is evidence that the rate of detection of intrauterine infection is higher when molecular microbiologic techniques are used [17-24] or when cultures are obtained from the chorioamniotic space [25].

Recent evidence indicates that intra-amniotic inflammation is also a risk factor for impending preterm delivery, as well as short- and long-term morbidity [26-35]. Indeed, patients with intra-amniotic inflammation detected by elevated cytokines (e.g., IL-6) [32], matrix-degrading enzymes (e.g., MMP-8) [36,37], or an amniotic fluid white blood cell count [36] have a similar prognosis to those with a positive culture for microorganisms. This underscores the importance of the rapid detection of intra-amniotic inflammation [37]. The optimal method for the diagnosis of intra-amniotic inflammation is rapid analysis of amniotic fluid obtained by amniocentesis. This is generally accomplished with the use of a Gram-stain, amniotic fluid white blood cell count, and amniotic fluid glucose [38,39]. The determinations of IL-6 and MMP-8 concentrations have proven to be sensitive and specific parameters for the identification of intra-amniotic inflammation [35-37,40].

The term “high-dimensional biology” refers to the use of high throughput techniques that allow simultaneous examination of changes in the genome (DNA), transcriptome (mRNA), proteome (proteins), or metabolome (metabolites) in a biological sample, with the goal of understanding the physiology or mechanisms of disease [41-43]. Insights derived from high-dimensional biology techniques are expected to assist with the development of new diagnostic, prognostic, and therapeutic tools in medicine [44]. Such techniques have included genomics [45-47], transcriptomics [48-74], proteomics [55,75-81], and metabolomics [82,83]. A critical aspect to this research strategy is the intelligent data mining of complex data sets generated with the use of these techniques, collectively referred to as “omics” sciences.

Examination of the amniotic fluid proteome has been employed as a means to identify biomarkers for intra-amniotic inflammation and those that may be useful in predicting the outcome of preterm labor [75-77,79,80]. The purpose of this study was to combine a novel computational method of pattern discovery with the use of mass spectrometric proteomic profiling of amniotic fluid to discover biomarkers of intra-amniotic inflammation. A key

element of the approach is to obtain a broadly inclusive proteomic profile using multiple simultaneous conditions in the acquisition of the mass spectrometric data, and to recombine these multiple conditions in a single, computationally efficient proteomic "fingerprint." A requirement of this fingerprint representation is its ability to represent all mass spectral features simultaneously for purposes of pattern discovery.

Materials and methods

A retrospective cross-sectional study was designed to include patients who presented with preterm labor and intact membranes and underwent amniocentesis for the evaluation of the microbial state of the amniotic cavity and/or fetal lung maturity. Amniotic fluid discarded for clinical purposes was collected, stored, and used for proteomic analysis.

Study population

Patients admitted after a diagnosis of preterm labor and intact membranes were asked to participate in a prospective cohort study designed to examine the relationship between clinical, biochemical, and biophysical parameters and the risk of preterm delivery, intrauterine infection and neurological disabilities. For the purposes of this study, we selected patients in this cohort who met the following criteria: (1) singleton gestation; (2) gestational age between 22 and 35 weeks and a live fetus; (3) cervical dilatation ≤ 3 cm by digital examination; (4) intact membranes; and (5) signed informed consent approved by the Institutional Review Board of the Sotero del Rio Hospital Santiago, Chile, Wayne State University Detroit, Michigan, and the *Eunice Kennedy Shriver* National Institute of Child Health and Human Development, NIH. Seventy-nine patients in this study were also included in an investigation conducted to explore the relationship between cervical length, vaginal fetal fibronectin, and preterm delivery.

Definitions, study procedures, and clinical management

Preterm labor was diagnosed in the presence of regular uterine contractions of at least 3 in 30 minutes, with or without cervical modifications. Beta-mimetic agents or magnesium sulfate were given intravenously for tocolysis, and steroids were administered between 24 and 34 weeks. An amniocentesis was performed trans-abdominally to assess the microbiological state of the amniotic cavity. The fluid was transported to the laboratory in a capped plastic syringe and cultured for aerobic and anaerobic bacteria, as well as genital mycoplasmas.The white blood cell (WBC) count, glucose concentration, and Gram stain for microorganisms were also obtained from the amniotic fluid.

Intra-amniotic infection and inflammation were defined as a positive amniotic fluid culture for microorganisms or an amniotic fluid IL (interleukin)-6 concentration >2600 pg/ml [32], respectively. The presumptive diagnosis of microbial invasion of the amniotic cavity/intra-amniotic inflammation was an indication for discontinuation of tocolysis at all gestational ages, and for administration of parenteral antibiotics until delivery.

Steroid administration (Betamethasone or Dexamethasone) was used regardless of the presumptive diagnosis of amniotic fluid inflammation, except in patients who had evidence of fetal lung maturity, as determined by a shake test and/or lamellar body count. After the 32nd week of gestation, patients with presumptive microbial invasion of the amniotic cavity/intra-amniotic inflammation who remained pregnant after 48 hours underwent augmentation of labor when required. In patients with intra-amniotic infection/inflammation before the 32nd week, management consisted of antibiotic administration without tocolysis. Clinical chorioamnionitis was an indication for augmentation of labor.

Amniotic Fluid Proteomic Profiling—Proteomic analysis of amniotic fluid samples was conducted using a combination of solid chromatography and mass spectrometry. Solid chromatography was performed using protein chips (Ciphergen Biosystems, Inc., Fremont, CA, USA). We used Surface Enhanced Laser Desorption Ionization-Time of Flight (SELDI-TOF) for mass spectrometry analysis (Ciphergen Biosystems, Inc., Fremont, CA, USA).

Amniotic fluid from each patient was diluted in sterile phosphate-buffered saline (PBS; 1.7mM KH_2PO_4, 5mM Na_2HPO_4, 150mM NaCl, pH 7.4) at a 1:10 dilution and placed on the protein chips selected for this study. Two types of protein chips were utilized, weak cation exchanger (CM10) and reversed phase (H50), to detect a wider range of the amniotic fluid proteome than could be detected with a single surface. The CM10 protein chip array incorporates a carboxylate chemistry (negatively charged) and, therefore, acts as a weak cationic exchanger, binding on its surface proteins or peptides which are positively charged at a given pH. The H50, or reversed phase, binds protein based upon hydrophobic interaction chromatography, which has binding characteristics similar to that of a C6 to C12 alkyl chromatographic resin. Protein or peptide separation on this surface is based upon hydrophobicity. Those with less hydrophobic content relative to the binding buffer will not bind to the array surface. Amniotic fluid samples were assayed in duplicate. One spot in every protein chip array was used to profile pooled midtrimester amniotic fluid to serve as an internal, experimental control.

Protein chip array preparation

H50 or CM10 protein chip arrays were placed in a bioprocessor (Ciphergen Biosystems Inc., Fremont, CA, USA), a device that allows the placement of 12 chips in a 96 well format. Chips were pre-washed twice with 50 microliters of 50% methanol for 5 minutes. The chip array was decanted, and 150 microliters of binding buffer (H50 binding buffer; 10% acetonitrile, 0.1% trifluoroacetic acid (TFA), or CM10 binding buffer; 10 mM Sodium Acetate, pH 4.0) was added to each spot on the array and incubated for 5 minutes, during which vigorous shaking was performed employing an automated microtiter plate shaker (Lab-line Instruments, Inc., Melrose Park, IL, USA). This step was performed twice to equilibrate the chip surface. Then, 50 microliters of diluted amniotic fluid samples were added to the protein chip arrays and incubated with vigorous shaking for 60 minutes. The samples in the wells were decanted, and the protein chip array was washed three times using 150 microliters of binding buffer for 5 minutes each. Finally, the protein chip array was washed with 150 microliters of de-ionized (DI) water, which was removed immediately. The protein chip arrays were then removed from the bioprocessor and allowed to air-dry for 5-10 minutes before the application of energy-absorbing molecules (EAM) or matrix.

Preparation and application of Energy Absorbing Molecules (EAMs)

Two different EAMs were utilized in this study to enlarge the mass range of protein detection: Cyano-4-hydroxycinnamic acid (CHCA), and Sinapinic acid (SPA). Two hundred microliters of 50% acetonitrile in 0.25% trifluoroacetic acid (TFA) were added to 5 milligrams of CHCA powder in a polypropylene tube and vortexed at room temperature (RT) for 5 minutes. Following the incubation, the tube was centrifuged for 15 minutes at 12,000x *g* at RT. The supernatant was removed and diluted with equal volume of 50% acetonitrile and 0.25% TFA prior to use. To prepare SPA, 400 μl of 50% acetonitrile in 0.5% TFA was added to a polypropylene tube containing 5 milligrams of SPA and vortexed for 5 minutes at RT. The SPA tube was centrifuged at 12,000x *g* for 15 minutes and the supernatant was retrieved for use. One microliter was applied to each protein chip array spot and allowed to air dry. This was followed by the addition of another microliter of the prepared EAMs.

Data acquisition

ProteinChip arrays were read on the Ciphergen PBS IIC instrument equipped with a ProteinChip array autoloader (ProteinChip software version 3.2) and exported to Ciphergen Express Data Manager software (version 3.0). Each protein chip array was read twice (at low- and high-laser energies). The mass spectrometer was calibrated using external mass standards (Calibrants: Arg8-Vasopressin, somatostatin, bovine insulin b-chain, human insulin, hirudin, bovine cytochrome C, equine myoglobin, carbonic anhydrase, enolase, bovine albumin, and bovine immunoglobulin).

For protein chip arrays containing CHCA as EAM, the mass scan was set to 0-100,000 Da for both low- and high-laser energy, and optimized from 3,000 – 10,000 Daltons. Low laser intensity was adjusted to a setting of 170 arbitrary laser units and high laser intensity was set at 185 arbitrary laser units. The mass deflector was adjusted to 500 Daltons for both low and high laser intensities. For protein chip arrays containing SPA as EAM, the mass scan was set to 0-200,000 Da for the low laser energy (200), and optimized from 3,000 – 10,000 Daltons. For high laser energy (220), the mass scan was optimized for 10,000-30,000 Da. The mass deflector was set at an automatic setting for protein chip arrays with SPA as matrix. The data acquisition method for all of the protein chip arrays was set to the SELDI quantitation setting.

Analysis of Mass Spectrometry Data—The purpose of proteomic profiling is to generate a description of the molecular composition of a biological fluid—in the present case, amniotic fluid. A given mass spectrometry tracing is, however, only one of many possible representations of the composition of the fluid in question. Other factors that can influence such a tracing include the clinical condition, controlled experimental variables (protein chip, EAM, laser intensity, etc.), as well as other unknown factors (experimental or otherwise). Data analysis is aimed at extracting relevant information in an unbiased way through the discovery and identification of biomarkers that allow the classification and prediction of clinical conditions.

Several approaches to the analysis of proteomic mass spectrometry data have been used [84-88]. We have developed a novel computational approach that overcomes some of the obstacles and limitations of previous methods. This technique discovers patterns which are combinations of spectral features (peaks). A unique characteristic of our method is the use of ensembles of patterns from all possible groupings of samples to construct a classification score. This score can, in turn, be used to classify the samples which meet the traditional definitions of health and disease and, potentially, discriminate intermediate phenotypes as well. A second attribute of this technique is that no *a priori* constraint need be placed on the number of features that comprise a pattern.

This method encompasses three broad components: first, signal transformation of the mass spectra into a tractable representation suitable for the discovery of patterns; second, the discovery of a set of patterns from the transformed signals, and third, a phenotypic classification scheme based on the set of patterns. Through a sequence of operations described briefly below and in detail in the Supplementary Materials, signal transformation reduces a set of mass spectra to a binary matrix. The rows in this matrix correspond to the mass spectra representing an individual patient sample, to which we often refer as an “instance.” The columns of the matrix correspond to the set of features selected from the mass spectra. This matrix forms the input to the pattern discovery algorithm.

Signal transformation comprises a number of steps which include: (a) pre-processing of the mass spectrum signals, (b) peak detection, (c) amplitude standardization, (d) encoding of the signals as binary “fingerprints,” (e) noise reduction, and (f) fusion of fingerprints across experimental conditions. Pattern discovery utilizes this representation of the set of signals to

produce a set of patterns which are then selected based on their information content relative to phenotypic class. The classification methodology using a repetitive training and testing procedure is based on a method of bootstrapping [89,90] that allows for the unbiased selection of parameters. A final blinded validation step is used to confirm that the pattern-based prediction results are generalizable (i.e. the model is not overtrained).

Signal transformation (see Figure 1)

Signal pre-processing

Mass spectrometry data are recorded as digital signals of amplitude (vertical axis) versus *m/z* (horizontal axis) (see Figure 2). Accordingly, standard digital signal processing may be applied [91,92]. The ultimate goal of this step is to obtain a computationally efficient representation of the signals that preserves all of the informative features. Signal processing consists of the following four steps described in detail below: 1) interpolation to a common horizontal axis; 2) removal of a background "trend"; and 3) averaging of duplicate spectra. Signal processing was implemented in MATLAB® software (The MathWorks, Inc., Natick, MA, USA) and the Perl programming language. Details of the procedure are provided in Supplementary Materials. Supplementary Materials.

Peak selection

Pattern discovery was performed using peaks detected in the spectra, the rationale being that biomarkers have only been chemically identified from spectral peaks and not from the baseline. Thus, the utilization of peaks for this purpose is consistent with this study's ultimate goal. We employed a two-step strategy comprising (a) detecting a large number of peaks including very weak ones, and (b) filtering peaks using a statistically-motivated peak selection strategy. The aim of this approach was to retain peaks which though small in amplitude nevertheless have the potential to contribute to informative patterns.

Amplitude Standardization of mass spectra

Mass spectrometry signals are inherently semi-quantitative in that no simple relationship exists between peptide/protein concentration and the amplitude of the peak in the mass spectra. Thus, to find patterns shared among subsets of an entire set of amniotic fluid samples, it is necessary to standardize the amplitude of the signals, a process sometimes referred to as "normalization." The method we employed is a variant of histogram equalization [93] that assigns the rank value of each peak as its standardized amplitude and, thus, preserves the peak-height rank relationships (shortest to tallest) within a spectrum.

Encoding Data for Pattern Discovery

Pattern discovery algorithms can be divided into those that operate in continuous-valued spaces and those that operate in discrete (or categorical) spaces. A categorical approach has the advantage over continuous representations of associating similar amplitude values of the mass spectra into a finite number of meaningful labels (e.g. "small," "medium" and "large" peaks). In contrast, working with continuous variables representing amplitude values of peaks generates potentially infinite subdivisions of the data, and this could obscure the recognition of informative patterns. Our pattern discovery algorithm requires a categorical representation of mass spectra. This approach enables identification of *all* patterns common to *all* subsets of patients, as will be described.

The simplest categorical representation of the mass spectrometry amplitudes is binary, with a "0" or a "1" representing the absence or presence of a feature. A more quantitative representation may be obtained by grouping amplitude values into categorical variables representing a finite set of ranges ("bins"). Transforming these categorical variables into a

binary representation is then simple. For example, given four bins, these values can be represented as: 000, 001, 010, 100. Each group of three digits represents a bin. While this is not an efficient binary representation of three categories, the use of bits (binary features described as 0 or 1) in the manner described ("indicator variables") is useful for pattern discovery. Table I shows the assignment of bits for this specific encoding using three thresholds for amplitude, T1, T2, and T3.

The encoding just described is referred to as "differential binning," since a bit is set for an amplitude value of the mass spectra contained within a given range. Mass spectrometry signals are better represented by "cumulative binning" in which successive bits are set for each sequential threshold that is exceeded by an amplitude value. Table II shows an example of this encoding scheme.

Since mass spectrometry is inherently semi-quantitative, there are situations where a peak is small in one spectrum, while larger in a corresponding spectrum from another patient, and yet the fact that both spectra have corresponding peaks is an important piece of information for pattern discovery. Cumulative binning preserves this relationship where differential binning may not. In order to capture this type of information, this study employs cumulative binning.

Given the rank-based method of standardization of the mass spectra described above, the "rank thresholds" form categories (bins) corresponding to percentiles. For example, given three thresholds at 50^{th}, 75^{th} and 95^{th} percentiles, standardized amplitude values below the 50^{th} percentile would not set any bits (e.g. "000"). Values above the 50^{th} and below the 75^{th} percentile would set the lowest bit ("001"). Values above the 75^{th} and below the 95^{th} percentiles would additionally set the next bit ("011") and, finally, values above the 95^{th} percentile would set all bits ("111"). Each peak, encoded in this way, generates several bits. The concatenation of all of these bits together forms a string of bits, or a "fingerprint."

Treatment of noise

A major challenge in the analysis of mass spectrometry data is the treatment of signal and noise. Important information may be contained not only in large amplitude peaks, but in small amplitude peaks as well. Thus, allowing small peaks to be present in the representation of the mass spectra is desirable. This has the potential disadvantage of overwhelming the analysis with noise. We handle this by constructing a "bit filter," requiring that, *within the training data only*, a bit occur more frequently in the spectra of one clinical group than in the other. This bit filter, found using only training data, was applied to both training and test datasets in order to construct a consistent set of fingerprints. We emphasize that this procedure is blinded to the clinical class of the test data (and also to the validation data) to be predicted. In the course of multiple training/testing experiments described below in the section on "Empirical modeling methodology," we found that a bit frequency ratio of 7 allowed us to find information-rich patterns without being overwhelmed by noise.

Fusion of fingerprints across experimental conditions

As described in the section on amniotic fluid proteomic profiling, there were eight experimental conditions for each amniotic fluid sample (two for protein chips (CM10 or H50), two for matrix (CHCA or SPA), and two for laser intensity (Low or High)). Each experimental condition contains different information. A particular advantage of the methods used in the present study is the ability to combine information from multiple experimental conditions of the same samples into a unified representation. Patterns comprised of information from disparate experimental conditions are therefore able to emerge and be found. Thus, mass spectra for each amniotic fluid sample from each experimental condition were subjected separately to binary

encoding, as described in the previous section. The resulting individual fingerprints were concatenated to form a single binary fingerprint for each amniotic fluid sample.

Pattern Discovery—The method of pattern discovery used in the present study is deterministic (i.e. non-heuristic) and complete. Because the method is based on a categorical representation of mass spectra, it is able to compute all possible clustering of the instances based on their fingerprints, and it can thus be said to be "complete". That is, each combination of instances gives rise to at most one pattern. Any subset of instances giving rise to a pattern is a cluster. Many patterns associated with such clusters are uninformative in identifying a particular phenotype because the protein composition of amniotic fluid has sources of variation having nothing to do with the phenotype of interest. In contrast, some patterns are highly informative. The pattern of proteins/peptides associated with each "pure" cluster (i.e. one which is strictly comprised of part of a single clinical phenotype) allows the generation of a testable hypothesis (i.e. does a distinct molecular phenotype have a distinct set of clinical correlates indicated by that pattern?). For example, among patients with preterm labor and intra-amniotic inflammation there may be subsets of patients which could be identified by the proteomic profile. Even though these groups of patients meet the clinical definition of phenotype used in the study, their molecular profiles may provide information about neonatal outcome which was not part of the definition of clinical phenotype and yet is of crucial clinical importance. This methodological approach has substantial implications for the development of a molecular taxonomy and pathophysiology of disease for conditions that are currently only defined at a "syndrome" level (combinations of clinical presentation and basic laboratory tests). The mathematical description of the pattern discovery algorithm is detailed in the Supplementary Materials.

Classification

Pattern similarity and generation of a score

Pattern discovery finds all patterns in common between all subsets of amniotic fluid samples. The similarity of an unknown sample to clinical phenotypes can be determined in terms of the patterns of proteins/peptides (fingerprint features) that it shares with the fingerprints of samples in the training set of each phenotype. An efficient way to classify unknown samples is to discover patterns that occur between each unknown sample as well as those identified in the training set. This method finds all patterns that co-occur in each unknown sample and all combinations of amniotic fluid samples in the training data (and therefore whose phenotype is known to the algorithm). A "good" pattern discriminating between two phenotypic classes would match only training samples for one phenotype, while matching in none of the other phenotype. An ideal pattern would match in all of the training samples in one phenotype and in none of the training samples of the other phenotype.

We used information theory to assign a score to each pattern based upon the numbers of instances of each phenotype in which the pattern occurs. In a two-class problem such as the present one, scores range from +1.0 to -1.0; the former represents patterns which occur in patients with preterm labor/delivery with IAI, and in none of the patients with preterm labor and term delivery. An "unknown" patient may be scored by summing the pattern scores for all of the patterns comprising the model. A positive score for a patient results in its predicted classification as preterm delivery with IAI, while a negative score results in its predicted classification as preterm labor with term delivery.

Empirical modeling methodology

The goal of this work is the discovery of proteomic patterns that correlate with well-characterized clinical phenotypes. The approach involves first the discovery and selection of a set of patterns, and then the evaluation of the information content of the patterns. Once a set

of patterns is validated by determining its ability to predict phenotype in a blinded set of profiles of amniotic fluid samples, it is dissected into the set features of which it is comprised.

Our empirical modeling methodology employs a cross-validation approach based upon the well-known bootstrapping procedure [89,90]. The method involves the subdivision of the clinical samples into two subsets: training/testing and validation. Multiple random draws from the training/testing subset are used to determine parameters that define the "model," i.e. the collection of patterns that are informative with respect to the phenotype (also called "class"). In this case, the two classes are preterm delivery with IAI and full-term delivery (preterm labor with term delivery). Once the model has been determined, it is used to predict the phenotypes of a blinded set of samples that have been withheld from analysis, and termed the "validation set." Figure 3 is a flowchart of this procedure. Bootstrap cross-validation verifies that the classifier is not over-trained.

Training/testing and validation subsets were comprised of 75% and 25% of the total number of instances, respectively. In cases of unequal numbers of instances in the two classes, the training/testing subsets were balanced. For example, for the data considered in this study, the numbers of samples from patients with preterm delivery with IAI and preterm labor with term delivery samples were 60 and 59 respectively. Thus, the training/testing sets consisted of 44 samples of each class, while the validation sets consisted of 16 samples from patients with preterm delivery with IAI and 15 samples of preterm labor with term delivery. The training/testing set was further randomly subdivided multiple times into 2/3 training samples and 1/3 test samples. (i.e. 29 instances of each class were assigned to the train subset and 15 to the test subset.) Randomization was accomplished by assigning a pseudorandom number to each sample and then sorting on that number, using routines available in Excel™ (Microsoft, Inc., Redmond, WA).

Each classifier was evaluated using multiple random training/testing draws (typically 100). An overall measure of classification accuracy for the specific selection of parameters is indicated by the mean and the confidence intervals. In addition, since every sample in the training/testing set was utilized as an "unknown" test sample approximately 33 times (1/3 of 100 draws), a statistical measure of the average classification accuracy for each test instance was also obtained.

After the optimal set of parameters defining a classifier was determined, this classifier was trained on the aggregate of the 44 samples from patients with preterm delivery with IAI and 44 from those with term delivery. The resulting classifier was used to predict the phenotypes of 16 patients with preterm delivery with IAI, and 15 patients with term delivery in the validation phase of the study. The performance of the classifier was evaluated using Receiver Operator Characteristic (ROC) curves.

Results

This study included patients with preterm labor who delivered at term (n=59) and those who delivered preterm with intra-amniotic infection/inflammation (n=60). The demographic and clinical characteristics of the patients included in the training/testing phase, as well as those included in the validation phase of the study, are described in Tables III and IV, respectively. The gestational age at amniocentesis was not significantly different between the term and preterm delivery groups.

The microorganisms isolated among patients with preterm labor and inflammation in the training/testing phase included: Ureaplasma urealyticum (n=16), Candida albicans (n=4), Fusobacterium sp. (n=2), Streptococcus sp. (n=1), Streptococcus agalactiae (n=1), Escherichia coli (n=1), Mycoplasma hominis (n=1), Listeria monocytogenes (n=1), Gardnerella vaginalis

(n=1), Peptostreptococcus sp. (n=1), Streptococcus viridans (n=1). More than one microorganism was identified in 8 patients, while no microorganism was isolated in 6 patients. The microbial and inflammatory status of the amniotic fluid in patients with preterm labor with intra-amniotic infection/inflammation included in the validation phase is depicted in Table V.

Classification of patients based on their associated SELDI-TOF mass spectra as belonging to either the class of patients with preterm delivery with IAI or term delivery was accomplished by constructing an empirical model using patterns discovered from training data. The first phase in the construction of this empirical model involved the selection of adjustable parameters utilizing the training/testing subset of data. The second phase tested the generalization of the model by utilizing the blinded validation set of instances that were not employed in parameter selection.

Training/testing Results

Most of the parameter choices relate to the conversion of mass spectra to binary fingerprints, as discussed previously. Many different values of parameters were explored during the training/testing process. We found that the classification results were fairly robust with respect to variations in encoding parameters, which is a good indication of how well the method should generalize the data outside the training/testing dataset. As discussed in the preceding section, we chose percentile binning and cumulative encoding. The important parameters associated with this method are the number and values of the thresholds for the quantization of amplitude bins. The best results were obtained with three quantization bins at percentile thresholds of 80%, 89.5%, and 99%. An additional parameter was the bit filter used for noise reduction, also as discussed above. For the best classification result, we required that the probability of a bit occurring in one phenotypic class be seven times greater than in the case of the other class. Utilizing these parameter choices, classification accuracies (averaged over 100 random draws) were: 91.4% (40.2/44) for patients with preterm delivery with IAI and 91.2% (40.1/44) for term delivery. In our exploration of parameter space, we observed that only a small set of the patients were consistently misclassified, whereas most patients were always classified correctly. Thus, the classification accuracy was dominated by a small number of ambiguous instances. This issue will be discussed in more detail below.

Validation Phase

Using the same encoding scheme and parameters as had been decided at the conclusion of the training/testing phase, pattern discovery and scoring were performed on the 16 patients with preterm delivery with IAI and 15 of those with term delivery that were withheld as validation data. The validation phase resulted in correct classification of 14 of the patients with preterm labor/delivery with IAI and 14 of those with preterm labor without IAI who delivered at term. Because of the small number of validation instances, a single instance carries much weight. Thus, the classification accuracy of the validation phase is consistent with the accuracies predicted from the training/testing phase. Table VI presents the results of the validation phase in the form of a confusion matrix. The overall accuracy was 90.3% (28/31).

The performance of the pattern-based classification can be illustrated using a ROC curve. Figure 4 shows the ROC curves for the validation set alone, as well as for the average in the case of the training/testing experiments over the 100 random draws described above. The fact that the validation results correspond closely with the training/testing results is indicative that the model is not over-trained.

The ROC curves display the relationship between sensitivity and specificity. However, our method uses objective criteria for the selection of the cutoff, namely, that positive scores

correspond to preterm labor/delivery with IAI classification and negative scores to preterm labor who delivered at term (see Figure 4 for details).

Discussion of misclassified patients

Misclassification was dominated by a few patients. To examine this, we un-blinded the validation data and ran the multiple random draw procedure on the entire data set. The same samples from patients with preterm labor/delivery with IAI from the training/testing random draws were misclassified along with two additional ones from the validation set. We examined the laboratory data for these patients and discovered that most misclassified patients had amniotic fluid white blood cell counts and IL-6 concentrations that were lower than average for the patients with preterm labor/delivery with IAI. It is therefore not surprising that these looked somewhat more like those with preterm labor and term delivery in their patterns. In general, a correlation exists between the score we calculate and these variables. Figure 5 shows scatter plots of the amniotic white blood cell count and IL-6 concentration versus the pattern-based score derived from proteomic analysis of AF.

Biomarkers—The goal of the present work was to discover novel markers, or novel patterns of markers indicative of preterm labor with intra-amniotic inflammation or infection. Classification accuracy, therefore, was used to determine the information content present in our representation of the data, as well as in individual spectral features (or combinations thereof) with respect to clinical outcome, in this case, preterm labor/delivery with IAI versus full-term delivery. Consequently, following completion of the classification studies described above, a search for informative markers and analogous patterns was undertaken. We found several statistically dominant peaks. In order to see beyond these, the search for markers was conducted iteratively, with the removal of significant features from previous iterations prior to the next iteration. Rank thresholds were adjusted downward at each one of the iterations in order to increase the detection sensitivity.

Table VII summarizes the result of this procedure. In all, 39 peaks in the fused spectra were determined in two iterations to carry significant information that collectively discriminates patients with preterm labor/delivery and IAI from those with preterm labor and term delivery.

Figure 6 displays the experimental data as a heat map. In this figure, the panel representing each of the 8 experimental conditions is divided into two parts. The upper section shows the data for samples from patients with preterm labor and term delivery, while the lower part demonstrates the data for the samples from patients with preterm labor/delivery with IAI. The figure shows the data between 2.5 kDa and 30 kDa, since this domain contained all of the significant informative markers.

There are a number of locations in Figure 6 where differences between patients with preterm labor/delivery with IAI and those with term delivery are readily apparent upon visual examination. For example, there is a group of peaks in the vicinity of 3.5 kDa that is present in patients with preterm labor/delivery with IAI and absent in those who delivered at term. The peaks can be seen in 6 of the 8 experimental conditions (when using SPA as an EAM combined with high laser power there is no useable data below about 9.8 kDa). In order to visualize the markers identified in Table VII, their locations are marked in Figure 6, below the relevant experimental condition panel.

The degree to which the selected spectral features are able to discriminate patients with preterm labor/delivery with IAI from those with term delivery (that is, the information content of the pattern) was determined by clustering all 119 instances based upon the pattern of features. There were 69 spectral features corresponding to 39 *m/z* locations (the multiplicity is due to the fact that the same *m/z* feature was sometimes detected in multiple experimental conditions).

For each instance, a vector of 69 features was extracted and rank normalized in the same way as had been done for the construction of the binary fingerprints. Note that the ranking is based on the original set of peaks for each experiment rather than ranking the 69 selected features. The resulting 119 × 69 matrix is shown in Figure 7. A 119 × 119 similarity matrix was computed as the correlation coefficients of all of the feature vectors, and a dendrogram was then computed using hierarchical agglomerative clustering. The result is displayed adjacent to the feature matrix in Figure 7, color coded according to clinical outcome (red for preterm labor/delivery with IAI, green for preterm labor with term delivery). Based upon this representation, it is possible to select a clustering threshold that results in a sensitivity of 91.7% and a specificity of 91.5%. This outcome is consistent with the pattern-based supervised classification results reported above, indicating that the features included in this proteomic pattern effectively capture all of the information present in the ensemble of features used in the supervised analysis. Furthermore, this result is significantly better than an unsupervised classification outcome based upon the binary fingerprints utilizing all of the spectral features (data not shown), indicating that the selected significant features not only contain essentially all of the information present in the data, but also exclude a significant amount of noise, thus improving the discriminating ability of the reduced representation.

It may also be observed that a few of the features in Figure 7, notably ones below 5 kDa, are present in nearly all of the samples of preterm delivery with infection/inflammation. An argument for parsimony argument would suggest that only these features are required for accurate classification. However, it is also clear in Figure 7 that there are other associations among instances that are carried primarily by other features. For example, features in the 5-10 kDa range are prevalent among a subset (but not all) of the patients with infection/ inflammation, and absent from patients who delivered at term. Another set of features above 15 kDa are present in a different subset of patients with infection/inflammation but are less prevalent (but not absent) in the group who delivered at term. Interestingly, the second of these subsets has a mean IL-6 concentration that is 60% higher than the first subset ($P < 0.05$). Thus, although it is not necessary that all features be considered in order to obtain an accurate overall classification of the samples, the additional pattern-based features appear to parse the groups into subsets which may indicate a correlation between molecular signature and clinical phenotype.

Discussion

Principal findings of the study

1) Analysis of amniotic fluid with a combination of solid chromatography (protein chip) and SELDI allows the identification of mass spectrometry features which can distinguish patients with preterm labor with intra-amniotic inflammation from those with preterm labor without inflammation or infection who subsequently deliver at term; 2) informative features in the mass spectrometry tracings were obtained using a novel computational approach which reduces the complexity of the data and identifies individual features as well as patterns related to the clinical phenotype; 3) the classifiers were originally derived by utilizing a testing and training set of samples (supervised learning). However, a high degree of accuracy [overall accuracy 90.3% (28/31)] was obtained when the classifiers were applied to a validation set of samples in a blinded fashion; 4) analysis of the informative mass spectrometry features which distinguish patients with preterm labor and intra-amniotic inflammation indicated that 39 features were identified as potential biomarkers; 5) there was substantial redundancy in the classification accuracy based upon the 39 features taken individually; 6) some of the proteins/peptides have been previously identified in amniotic fluid of patients with intra-amniotic infection/ inflammation. However, most of the features reported herein remain to be identified; and 7) the computational approach described in this article has the potential to identify patterns of

informative features in this biological fluid. However, its application can extend beyond this matrix to vaginal/cervical fluid, blood, cerebral spinal fluid, urine, as well as other biological fluids.

Proteomic analysis of amniotic fluid in the preterm parturition syndrome

The amniotic fluid proteome is the entire set of proteins/peptides present in this biological fluid. A global description of the number of proteins, their concentrations, function, posttranslational modifications, as well as the protein/protein interactions in this fluid remains has not yet been described. An "amniotic fluid proteome project" is desirable to maximize the diagnostic and prognostic value of amniotic fluid analysis, as well as to understand the physiologic properties of this fluid.

Several efforts have been undertaken to characterize the protein composition of amniotic fluid [75-77,79,80]. Some aimed at determining the presence (or absence) of a particular protein, its concentration, and whether it changes with gestational age or pathologic states. The typical example of an informative protein is alpha fetoprotein, which has been employed in the diagnosis of neural tube defects [94] and other congenital defects [95]. Other investigators have used two-dimensional gel electrophoresis to provide a description of the protein composition of amniotic fluid [77]. Recently, proteomic techniques have focused on the identification of biomarkers for intra-amniotic inflammation/infection in patients with preterm labor with intact membranes [75,76,79,80] and/or PROM [80].

Proteomic studies of complex biological fluids to identify biomarkers present two major challenges: analysis of fluid composition with biochemical techniques (SELDI, MALDI, 2D electrophoresis, etc.) and data mining. We have used SELDI in this study because of its early promise in the identification of biomarkers. The data mining approach employed herein was selected because of its ability to discover patterns of features that have the potential to be more informative than a single individual pattern. Moreover, this approach has the theoretical strength to identify patterns capable of segregating patients with "intermediate phenotypes." This approach is deterministic and complete, and these are major advantages over probabilistic and/or heuristic computational methods.

SELDI

Methods for discovering proteomic biomarkers are diverse and controversial. There is no consensus yet regarding a preferred methodology. One axis of discussion relates to the tradeoff between the throughput of a method and its depth/breadth of coverage of the proteome. The present work has employed SELDI-MS, which is broadly regarded as a high-throughput method for proteomic profiling, but one that sacrifices proteomic coverage. In an effort to find a middle ground between throughput and coverage, we have chosen to combine multiple "dimensions" of SELDI-MS. That is, we have used multiple combinations of chromatographic surfaces, energy-absorbing matrices, and laser intensities. Each combination produces a different picture of the proteome of amniotic fluid. The fusion of data across multiple SELDI dimensions creates a more comprehensive view of the proteome. Newly available methods for proteomic profiling have improved capabilities to identify and quantify proteins (e.g., iTRAQ). The theoretical advantages over SELDI of such technologies are appealing.

Computational analysis

The computational method described in this article focuses on the identification of mass spectrometric patterns. The idea that combinations of protein markers may be more informative with respect to diagnosis of disease than any one marker is gaining broader acceptance [96-101]. The analytical methods described in the present work were carefully designed to detect the presence of such informative combinations, even if their proteomic constituents are

not individually revealing. In order that such subtle, yet potentially important patterns be detectable, it is not sufficient to perform statistical analysis of individual *m/z* locations, individual peaks, individual SELDI dimensions, or any other apportioning of the available data. Rather, it is necessary to first combine all of the data into a comprehensive summary in which all potential biomarkers have a comparable representation, and then seek informative combinations of features within this fused representation.

Previous work in biomarker-based prediction of preterm labor associated with inflammation and/or infection has succeeded in achieving prediction accuracies comparable to those reported here. Therefore, the objective of this work was to detect biomarkers and determine whether present patterns of biomarkers for the identification of preterm labor are associated with inflammation. In that regard, the use of a deterministic and complete algorithm, combined with an efficient fingerprint representation of arbitrary-dimensionality mass spectrometry data, has a number of attractive attributes. First, because patterns are discovered without bias towards a small number of features that may have dominant individual statistical influence, other features are given an equal opportunity to form highly informative patterns regardless of their individual informativeness. Second, because the method is deterministic, it is straightforward to apply it iteratively, removing biomarkers and patterns discovered in previous iterations in order to reveal additional informative features. This approach may have important implications for the understanding of the mechanisms of disease, although it may have limited diagnostic or prognostic value.

Proteomic Analysis for the identification of intra-amniotic inflammation/infection

The present study was designed to identify features distinguishing women with preterm labor and intact membranes with intra-amniotic inflammation/infection from those with preterm labor who do not have evidence of inflammation and deliver at term. This was a case-control study planned to maximize discovery of features associated with inflammation. Training and testing methodology was used to develop a model capable of accurately classifying disease vs. non-disease. The value of the classifiers was tested in a separate set of samples (i.e., validation set). The overall accuracy in the validation set was 90.3% (28/31), while in the training/testing set the result was 91% (80/88). These results suggest that the classifiers generated by the model will generalize the prospective samples, provided that they belong to the same parent populations and that their proteomic profiles are generated identically. Our results are in keeping with those reported by other investigators [75,79] conducting proteomic analysis of amniotic fluid.

Classification errors

Three out of 31 patients were misclassified in the validation set. Two patients had intra-amniotic inflammation/infection (see Table V, patients 4 and 13), but were not identified as such by proteomic profiling. One patient had a positive culture for E.coli, an elevated amniotic fluid white blood cell count (310 cells/mm^3), elevated IL-6 (69 ng/ml), and a low glucose (9 mg/dL). The second patient had an infection with fungi, an elevated white blood cell count (280 cells/mm^3), an elevated IL-6 (14.4 ng/ml) and a low amniotic fluid glucose (1 mg/dl). Therefore, these patients have strong evidence of a false negative result by proteomic profiling.

One patient had an episode of preterm labor with intact membranes at 31 weeks of gestation, had a negative amniotic fluid culture for bacteria, no amniotic fluid white blood cells, an IL-6 of 1.1 mg/mL, and an amniotic fluid glucose of 30 mg/dl. This patient remained undelivered until 39 weeks, and gave birth to a neonate that weighed 2950 grams. Thus, this patient represents a false-positive amniotic fluid proteomic profile. The possibility exists that there was a transitory inflammatory process detected by proteomic profiling of AF which was missed by conventional tests. However, we have no evidence for this.

Our interpretation of examining false-positive and false-negative results of proteomic profiling of AF in the validation set of samples is that this technique is not immune to diagnostic errors. Further studies are required to explain this situation.

m/z ratios of informative mass spectrometry features

The model developed for classification purposes could be mined for informative features. We identified 39 unique *m/z* features from across the 6 different experimental conditions (2 protein chips, 2 energy-absorbing materials or matrices, and 2 laser intensities). Table VII presents the *m/z* ratio of informative features. Some of these have been previously reported, while others are novel. The table describes the experimental conditions under which the peaks were identified. A glance at the table indicates the cationic protein chip yields more informative peaks than the hydrophobic chip.

Strengths and limitations of the study

The strengths of the study are that it employed two protein chips (hydrophobic and cationic) for chromatography, clearly characterized phenotypes using multiple tests (amniotic fluid culture, white blood cell count, amniotic fluid IL-6, and Gram stain of amniotic fluid), as well as a novel computational method. Limitations of this study include that it is a case control rather than a cohort design, the absence of a group of patients with preterm labor without inflammation who delivered preterm, and that protein identification of the informative features has not been provided at this time. Further studies are required to address these limitations.

The issue of the intermediate phenotypes

The classification of patients into two phenotypes (for example patients with preterm labor with intra-amniotic inflammation/infection vs. those without inflammation/infection who deliver at term) is useful in providing a framework to discover biomarkers. However, it is clearly an oversimplification of the biology of premature labor. While it is often possible to describe stereotypical phenotypes and then lump patients into one of two (or several) such possibilities, this approach usually breaks down under close scrutiny. Although two patients may be assigned to a single phenotype, it is invariably true that at some level there are differences between them, and in many cases these differences are important from the perspective of clinical management.

The traditional classification of the neoplastic state of the uterine cervix includes three distinct classes of patients: (1) those without any evidence of neoplasia (i.e. healthy); (2) those in whom neoplastic cells are limited to the epithelium and, therefore, have carcinoma *in situ*, and (3) those in whom neoplastic cells have invaded the basement membrane and, thus, have invasive cervical cancer. Generally, high-dimensional biology has focused on the extreme phenotypes composed of healthy women and those with invasive cancer. This approach ignores the biological (and clinical) reality of patients with carcinoma in situ who represent an "intermediate phenotype."

In the context of premature labor and intrauterine infection/inflammation, a similar spectrum of disease can be considered. At least three groups of women can be identified: 1) women with premature labor and no microorganisms in the amniotic fluid who deliver at term; 2) those with microbial invasion of the amniotic cavity with a high microbial burden and severe inflammation who deliver shortly after admission; and 3) one or more intermediate groups in which there is some degree of intra-amniotic inflammation. Milder degrees of inflammation in comparison with group 2 may represent an early phase of microbial invasion of the amniotic cavity in which the host has not had time to deploy an inflammatory response, patients who are unable to mount an inflammatory response even in the presence of a high microbial burden, or patients who have been examined after the microbial invasion has been controlled by an appropriate

inflammatory response. The molecular profile of each distinct intermediate phenotype will predictably vary between patients who delivered at term and those with severe infection/inflammation. Moreover, there will presumably be molecular heterogeneity within the intermediate phenotypes. The pressing need to identify, classify, predict and treat intermediate phenotypes underlies our effort to develop new computational approaches to the analysis of high-dimensional biology which is described in Material and Methods section of this study.

The concept that patterns of features represent clusters of patients and that ensembles of patterns provide a basis for classifying patients into distinct phenotypes may be revisited in the context of "intermediate phenotypes." A "perfect" pattern in the hypothetical "ideal world" of the two extreme phenotypes "diseased" and "healthy" would be one that only occurs in one of the two phenotypes and, furthermore, one that occurs in every patient that is a true member of that phenotype. However, in clinical practice this situation is rarely the case. This might be regarded as a failure of biomarker discovery due, for whatever reason, to a lack of correlation between experimental observation and clinical outcome. Another point of view, however, is that this phenomenon is the direct result of the phenotypic heterogeneity among patients that occurs in spite of stringent selection criteria, which, after all, are based on preconceived phenotypic views. We propose that this heterogeneity may be accurately reflected in molecular "fingerprints" and, therefore, would enable the creation of a molecular taxonomy of the disease (s). Such a taxonomy would provide a more detailed, informative and, hopefully, useful, classification of patients.

In the present study no such "perfect" patterns were observed. However, there is evidence of a relation between the pattern-based scoring function (which represents the degree of similarity of an instance with all clusterings of each phenotype) and clinical outcome variables (e.g. IL-6 and AF WBC as shown in Figure 5). As the pattern-based score increases there is an increased likelihood of extreme elevation of these variables, which may be regarded as a gradual approach towards an extreme phenotype — that of preterm delivery due for example to severe inflammation or high microbial burden.

It is important to note that the ability to find patterns in a proteomic profiling experiment that may be indicative of intermediate phenotypes must not depend on *a priori* knowledge of the intermediate phenotypes. Rather, robust informative patterns with partial support among the presumptive extreme phenotypes represent new hypotheses that should emerge from the analysis in a natural way. It is a case of "ask a simple question, get a complicated answer." In this case, the "complicated answer" represents new hypotheses that can be subsequently tested by seeking specific correlations distinguishing members of extreme phenotypes from members of intermediate phenotypes in clinically meaningful ways.

Conclusions

Proteomic profiling of amniotic fluid allowed the identification of 39 mass spectrometric features, which were collectively informative in distinguishing patients with preterm labor with intra-amniotic infection/inflammation from those with preterm labor who subsequently delivered at term. Some of the proteins/peptides that correspond to the 39 mass spectrometric peaks have been previously identified in amniotic fluid of patients with intra-amniotic infection/inflammation. However, most of the features reported herein remain to be identified.

Supplementary Material

Refer to Web version on PubMed Central for supplementary material.

Acknowledgements

The authors wish to acknowledge the contributions of the Nursing staff of the Perinatology Research Branch and Detroit Medical Center: Ms Nancy Hauff, Ms Sandy Field, Ms Lorraine Nikita, Ms Vicky Ineson, Ms Mahbubeh Mahmoudieh, Ms Julie McKinley, Ms Sue Rehel, Ms Shannon Donegan, Ms Linda Bouey, Ms Carolyn Sudz, Ms Sylvia Warren, Ms Shelley Mullen, Ms Gail Barley, Ms Denise Bayoneto, Ms Judy Kerman, Ms Barb Steffy, Ms Milagros Kitchen, and Ms Leandra Ga-Pinlac. The authors also wish to acknowledge Herb Holyst who wrote the heat graph visualization software as well as much of the software used to process the mass spectrometry data. The contributions of faculty, private physicians, residents, fellows, and nursing staff at the participating institutions is gratefully acknowledged.

This research was supported by the Intramural Research Program of the *Eunice Kennedy Shriver* National Institute of Child Health and Human Development, NIH, DHHS.

Reference List

1. Hack M, Fanaroff AA. Outcomes of extremely immature infants--a perinatal dilemma. N.Engl.J Med 1993;329:1649–1650. [PubMed: 8232435]
2. Dammann O, Leviton A, Gappa M, Dammann CE. Lung and brain damage in preterm newborns, and their association with gestational age, prematurity subgroup, infection/inflammation and long term outcome. BJOG 2005;112(Suppl 1):4–9. [PubMed: 15715586]
3. Leavitt RP, Green NS, Katz M. Current and future directions of research into prematurity: report of the symposium on prematurity held on 21-22 November 2005. Pediatr.Res 2006;60:777–780. [PubMed: 17065569]
4. Callaghan WM, MacDorman MF, Rasmussen SA, Qin C, Lackritz EM. The contribution of preterm birth to infant mortality rates in the United States. Pediatrics 2006;118:1566–1573. [PubMed: 17015548]
5. Moutquin JM. Classification and heterogeneity of preterm birth. BJOG 2003;110(Suppl 20):30–33. [PubMed: 12763108]
6. Tucker JM, Goldenberg RL, Davis RO, Copper RL, Winkler CL, Hauth JC. Etiologies of preterm birth in an indigent population: is prevention a logical expectation? Obstet Gynecol 1991;77:343–347. [PubMed: 1992395]
7. Richardson DK, Gray JE, Gortmaker SL, Goldmann DA, Pursley DM, McCormick MC. Declining severity adjusted mortality: evidence of improving neonatal intensive care. Pediatrics 1998;102:893–899. [PubMed: 9755261]
8. Yost CC, Soll RF. Early versus delayed selective surfactant treatment for neonatal respiratory distress syndrome. Cochrane.Database.Syst.Rev 2000:CD001456. [PubMed: 10796266]
9. Soll RF. Prophylactic natural surfactant extract for preventing morbidity and mortality in preterm infants. Cochrane.Database.Syst.Rev 2000:CD000511. [PubMed: 10796380]
10. Wen SW, Smith G, Yang Q, Walker M. Epidemiology of preterm birth and neonatal outcome. Semin.Fetal Neonatal Med 2004;9:429–435. [PubMed: 15691780]
11. Crowley P. Prophylactic corticosteroids for preterm birth. Cochrane.Database.Syst.Rev 2000:CD000065. [PubMed: 10796110]
12. Roberts D, Dalziel S. Antenatal corticosteroids for accelerating fetal lung maturation for women at risk of preterm birth. Cochrane.Database.Syst.Rev 2006;3:CD004454. [PubMed: 16856047]
13. Crowther CA, Hiller JE, Doyle LW. Magnesium sulphate for preventing preterm birth in threatened preterm labour. Cochrane.Database.Syst.Rev 2002:CD001060. [PubMed: 12519550]
14. Anotayanonth S, Subhedar NV, Garner P, Neilson JP, Harigopal S. Betamimetics for inhibiting preterm labour. Cochrane.Database.Syst.Rev 2004:CD004352. [PubMed: 15495104]
15. Grimes DA, Nanda K. Magnesium sulfate tocolysis: time to quit. Obstet Gynecol 2006;108:986–989. [PubMed: 17012463]
16. Goncalves LF, Chaiworapongsa T, Romero R. Intrauterine infection and prematurity. Ment.Retard.Dev.Disabil.Res.Rev 2002;8:3–13. [PubMed: 11921380]
17. Blanchard A, Hentschel J, Duffy L, Baldus K, Cassell GH. Detection of Ureaplasma urealyticum by polymerase chain reaction in the urogenital tract of adults, in amniotic fluid, and in the respiratory tract of newborns. Clin.Infect.Dis 1993;17(Suppl 1):S148–S153. [PubMed: 8399906]

18. Jalava J, Mantymaa ML, Ekblad U, Toivanen P, Skurnik M, Lassila O, Alanen A. Bacterial 16S rDNA polymerase chain reaction in the detection of intra-amniotic infection. Br J Obstet Gynaecol 1996;103:664–669. [PubMed: 8688393]
19. Hitti J, Riley DE, Krohn MA, Hillier SL, Agnew KJ, Krieger JN, Eschenbach DA. Broad-spectrum bacterial rDNA polymerase chain reaction assay for detecting amniotic fluid infection among women in premature labor. Clin.Infect.Dis 1997;24:1228–1232. [PubMed: 9195088]
20. Oyarzun E, Yamamoto M, Kato S, Gomez R, Lizama L, Moenne A. Specific detection of 16 micro-organisms in amniotic fluid by polymerase chain reaction and its correlation with preterm delivery occurrence. Am J Obstet Gynecol 1998;179:1115–1119. [PubMed: 9822484]
21. Yoon BH, Romero R, Kim M, Kim EC, Kim T, Park JS, Jun JK. Clinical implications of detection of Ureaplasma urealyticum in the amniotic cavity with the polymerase chain reaction. Am J Obstet Gynecol 2000;183:1130–1137. [PubMed: 11084554]
22. Bearfield C, Davenport ES, Sivapathasundaram V, Allaker RP. Possible association between amniotic fluid micro-organism infection and microflora in the mouth. BJOG 2002;109:527–533. [PubMed: 12066942]
23. Yoon BH, Romero R, Lim JH, Shim SS, Hong JS, Shim JY, Jun JK. The clinical significance of detecting Ureaplasma urealyticum by the polymerase chain reaction in the amniotic fluid of patients with preterm labor. Am J Obstet Gynecol 2003;189:919–924. [PubMed: 14586326]
24. Gardella C, Riley DE, Hitti J, Agnew K, Krieger JN, Eschenbach D. Identification and sequencing of bacterial rDNAs in culture-negative amniotic fluid from women in premature labor. Am J Perinatol 2004;21:319–323. [PubMed: 15311367]
25. Cassell GH, Andrews W, Hauth J. Isolation of microorganisms from the chorioamnion is twice that from amniotic fluid at cesarean delivery in women with intact membranes. Am J Obstet Gynecol 1993;168:A462.
26. Yoon BH, Romero R, Kim CJ, Jun JK, Gomez R, Choi JH, Syn HC. Amniotic fluid interleukin-6: a sensitive test for antenatal diagnosis of acute inflammatory lesions of preterm placenta and prediction of perinatal morbidity. Am.J.Obstet.Gynecol 1995;172:960–970. [PubMed: 7892891]
27. Yoon BH, Romero R, Kim CJ, Koo JN, Choe G, Syn HC, Chi JG. High expression of tumor necrosis factor-alpha and interleukin-6 in periventricular leukomalacia. Am.J.Obstet.Gynecol 1997;177:406–411. [PubMed: 9290459]
28. Yoon BH, Romero R, Jun JK, Park KH, Park JD, Ghezzi F, Kim BI. Amniotic fluid cytokines (interleukin-6, tumor necrosis factor-alpha, interleukin-1 beta, and interleukin-8) and the risk for the development of bronchopulmonary dysplasia. Am.J.Obstet.Gynecol 1997;177:825–830. [PubMed: 9369827]
29. Yoon BH, Romero R, Kim KS, Park JS, Ki SH, Kim BI, Jun JK. A systemic fetal inflammatory response and the development of bronchopulmonary dysplasia. Am J Obstet Gynecol 1999;181:773–779. [PubMed: 10521727]
30. Yoon BH, Romero R, Park JS, Kim M, Oh SY, Kim CJ, Jun JK. The relationship among inflammatory lesions of the umbilical cord (funisitis), umbilical cord plasma interleukin 6 concentration, amniotic fluid infection, and neonatal sepsis. Am J Obstet Gynecol 2000;183:1124–1129. [PubMed: 11084553]
31. Yoon BH, Oh SY, Romero R, Shim SS, Han SY, Park JS, Jun JK. An elevated amniotic fluid matrix metalloproteinase-8 level at the time of midtrimester genetic amniocentesis is a risk factor for spontaneous preterm delivery. Am J Obstet Gynecol 2001;185:1162–1167. [PubMed: 11717651]
32. Yoon BH, Romero R, Moon JB, Shim SS, Kim M, Kim G, Jun JK. Clinical significance of intra-amniotic inflammation in patients with preterm labor and intact membranes. Am J Obstet Gynecol 2001;185:1130–1136. [PubMed: 11717646]
33. Yoon BH, Romero R, Park JS, Kim CJ, Kim SH, Choi JH, Han TR. Fetal exposure to an intra-amniotic inflammation and the development of cerebral palsy at the age of three years. Am.J.Obstet.Gynecol 2000;182:675–681. [PubMed: 10739529]
34. Moon JB, Kim JC, Yoon BH, Romero R, Kim G, Oh SY, Kim M, Shim SS. Amniotic fluid matrix metalloproteinase-8 and the development of cerebral palsy. J Perinat.Med 2002;30:301–306. [PubMed: 12235718]

35. Shim SS, Romero R, Hong JS, Park CW, Jun JK, Kim BI, Yoon BH. Clinical significance of intra-amniotic inflammation in patients with preterm premature rupture of membranes. Am.J.Obstet.Gynecol 2004;191:1339–1345. [PubMed: 15507963]
36. Maymon E, Romero R, Chaiworapongsa T, Berman S, Conoscenti G, Gomez R, Edwin S. Amniotic fluid matrix metalloproteinase-8 in preterm labor with intact membranes. Am.J.Obstet.Gynecol 2001;185:1149–1155. [PubMed: 11717649]
37. Nien JK, Yoon BH, Espinoza J, Kusanovic JP, Erez O, Soto E, Richani K, Gomez R, Hassan S, Mazor M, et al. A rapid MMP-8 bedside test for the detection of intra-amniotic inflammation identifies patients at risk for imminent preterm delivery. Am.J.Obstet.Gynecol 2006;195:1025–1030. [PubMed: 17000236]
38. Romero R, Yoon BH, Mazor M, Gomez R, Diamond MP, Kenney JS, Ramirez M, Fidel PL, Sorokin Y, Cotton D, et al. The diagnostic and prognostic value of amniotic fluid white blood cell count, glucose, interleukin-6, and gram stain in patients with preterm labor and intact membranes. Am.J.Obstet.Gynecol 1993;169:805–816. [PubMed: 7694461]
39. Romero R, Yoon BH, Mazor M, Gomez R, Gonzalez R, Diamond MP, Baumann P, Araneda H, Kenney JS, Cotton DB, et al. A comparative study of the diagnostic performance of amniotic fluid glucose, white blood cell count, interleukin-6, and gram stain in the detection of microbial invasion in patients with preterm premature rupture of membranes. Am.J.Obstet.Gynecol 1993;169:839–851. [PubMed: 7694463]
40. Romero R, Yoon BH, Kenney JS, Gomez R, Allison AC, Sehgal PB. Amniotic fluid interleukin-6 determinations are of diagnostic and prognostic value in preterm labor. Am.J.Reprod.Immunol 1993;30:167–183. [PubMed: 8311926]
41. Evans GA. Designer science and the “omic” revolution. Nat.Biotechnol 2000;18:127. [PubMed: 10657071]
42. Gracey AY, Cossins AR. Application of microarray technology in environmental and comparative physiology. Annu.Rev.Physiol 2003;65:231–259. [PubMed: 12471169]
43. Mehta T, Tanik M, Allison DB. Towards sound epistemological foundations of statistical methods for high-dimensional biology. Nat.Genet 2004;36:943–947. [PubMed: 15340433]
44. Mitra AP, Lin H, Cote RJ, Datar RH. Biomarker profiling for cancer diagnosis, prognosis and therapeutic management. Natl.Med.J India 2005;18:304–312. [PubMed: 16483031]
45. Watanabe A, Cornelison R, Hostetter G. Tissue microarrays: applications in genomic research. Expert.Rev.Mol.Diagn 2005;5:171–181. [PubMed: 15833047]
46. Friel L, Kuivaniemi H, Gomez R, Goddard K, Nien JK, Tromp G, Lu Q, Xu Z, Behnke E, Solari M, et al. Genetic predisposition for preterm PROM: Results of a large candidate-gene association study of mothers and their offspring. Am.J.Obstet.Gynecol 2005;193:S17.
47. Romero R, Kuivaniemi H, Tromp G, Olson J. The design, execution, and interpretation of genetic association studies to decipher complex diseases. Am.J.Obstet.Gynecol 2002;187:1299–1312. [PubMed: 12439524]
48. Scatena CD, Adler S. Characterization of a human-specific regulator of placental corticotropin-releasing hormone. Mol.Endocrinol 1998;12:1228–1240. [PubMed: 9717848]
49. Tashima LS, Millar LK, Bryant-Greenwood GD. Genes upregulated in human fetal membranes by infection or labor. Obstet.Gynecol 1999;94:441–449. [PubMed: 10472875]
50. Tarca AL, Romero R, Draghici S. Analysis of microarray experiments of gene expression profiling. Am.J.Obstet.Gynecol 2006;195:373–388. [PubMed: 16890548]
51. Aguan K, Carvajal JA, Thompson LP, Weiner CP. Application of a functional genomics approach to identify differentially expressed genes in human myometrium during pregnancy and labour. Mol.Hum.Reprod 2000;6:1141–1145. [PubMed: 11101697]
52. Alizadeh AA, Eisen MB, Davis RE, Ma C, Lossos IS, Rosenwald A, Boldrick JC, Sabet H, Tran T, Yu X, et al. Distinct types of diffuse large B-cell lymphoma identified by gene expression profiling. Nature 2000;403:503–511. [PubMed: 10676951]
53. Muhle RA, Pavlidis P, Grundy WN, Hirsch E. A high-throughput study of gene expression in preterm labor with a subtractive microarray approach. Am.J.Obstet.Gynecol 2001;185:716–724. [PubMed: 11568803]

54. Chan EC, Fraser S, Yin S, Yeo G, Kwek K, Fairclough RJ, Smith R. Human myometrial genes are differentially expressed in labor: a suppression subtractive hybridization study. J.Clin.Endocrinol.Metab 2002;87:2435–2441. [PubMed: 12050195]
55. Romero R, Kuivaniemi H, Tromp G. Functional genomics and proteomics in term and preterm parturition. J.Clin.Endocrinol.Metab 2002;87:2431–2434. [PubMed: 12050194]
56. van de Vijver MJ, He YD, van't Veer LJ, Dai H, Hart AA, Voskuil DW, Schreiber GJ, Peterse JL, Roberts C, Marton MJ, et al. A gene-expression signature as a predictor of survival in breast cancer. N.Engl.J Med 2002;347:1999–2009. [PubMed: 12490681]
57. Weston GC, Ponnampalam A, Vollenhoven BJ, Healy DL, Rogers PA. Genomics in obstetrics and gynaecology. Aust.N.Z.J Obstet Gynaecol 2003;43:264–272. [PubMed: 14714710]
58. 't Veer LJ, Dai H, van de Vijver MJ, He YD, Hart AA, Bernards R, Friend SH. Expression profiling predicts outcome in breast cancer. Breast Cancer Res 2003;5:57–58. [PubMed: 12559048]
59. Tromp G, Kuivaniemi H, Romero R, Chaiworapongsa T, Kim YM, Kim MR, Maymon E, Edwin S. Genome-wide expression profiling of fetal membranes reveals a deficient expression of proteinase inhibitor 3 in premature rupture of membranes. Am.J.Obstet.Gynecol 2004;191:1331–1338. [PubMed: 15507962]
60. Merrick BA, Bruno ME. Genomic and proteomic profiling for biomarkers and signature profiles of toxicity. Curr.Opin.Mol.Ther 2004;6:600–607. [PubMed: 15663324]
61. Bisits AM, Smith R, Mesiano S, Yeo G, Kwek K, MacIntyre D, Chan EC. Inflammatory aetiology of human myometrial activation tested using directed graphs. PLoS.Comput.Biol 2005;1:132–136. [PubMed: 16110333]
62. Wilson RD. Genomics: new technology for obstetrics. J Obstet Gynaecol.Can 2005;27:63–75. [PubMed: 15937585]
63. Havelock JC, Keller P, Muleba N, Mayhew BA, Casey BM, Rainey WE, Word RA. Human myometrial gene expression before and during parturition. Biol.Reprod 2005;72:707–719. [PubMed: 15509731]
64. Huber A, Hudelist G, Czerwenka K, Husslein P, Kubista E, Singer CF. Gene expression profiling of cervical tissue during physiological cervical effacement. Obstet Gynecol 2005;105:91–98. [PubMed: 15625148]
65. Word RA, Landrum CP, Timmons BC, Young SG, Mahendroo MS. Transgene insertion on mouse chromosome 6 impairs function of the uterine cervix and causes failure of parturition. Biol.Reprod 2005;73:1046–1056. [PubMed: 16034000]
66. Haddad R, Tromp G, Kuivaniemi H, Chaiworapongsa T, Kim YM, Mazor M, Romero R. Human spontaneous labor without histologic chorioamnionitis is characterized by an acute inflammation gene expression signature. Am.J.Obstet.Gynecol 2006;195:394–24. [PubMed: 16890549]
67. Hassan SS, Romero R, Haddad R, Hendler I, Khalek N, Tromp G, Diamond MP, Sorokin Y, Malone J Jr. The transcriptome of the uterine cervix before and after spontaneous term parturition. Am.J.Obstet.Gynecol 2006;195:778–786. [PubMed: 16949412]
68. Bukowski R, Hankins GD, Saade GR, Anderson GD, Thornton S. Labor-associated gene expression in the human uterine fundus, lower segment, and cervix. PLoS.Med 2006;3:e169. [PubMed: 16768543]
69. Romero R, Tarca AL, Tromp G. Insights into the Physiology of Childbirth Using Transcriptomics. PLoS.Med 2006;3:e276. [PubMed: 16752954]
70. Haddad R, Gould BR, Romero R, Tromp G, Farookhi R, Edwin SS, Kim MR, Zingg HH. Uterine transcriptomes of bacteria-induced and ovariectomy-induced preterm labor in mice are characterized by differential expression of arachidonate metabolism genes. Am.J.Obstet.Gynecol 2006;195:822–828. [PubMed: 16949419]
71. Pennell CE, Oldenhof AD, Perkins JE, Dunk CE, Keunen J, Tan P, Bocking AD, Lye SJ. Identification of a Gene Expression Signature in Leukocytes that Predicts Preterm Delivery in Women with Threatened Preterm Labour. J.Soc.Gynecol.Investig 2006;13:175A.
72. Romero R, Tromp G. High-dimensional biology in obstetrics and gynecology: functional genomics in microarray studies. Am J Obstet Gynecol 2006;195:360–363. [PubMed: 16890547]
73. Ward K. Microarray technology in obstetrics and gynecology: a guide for clinicians. Am J Obstet Gynecol 2006;195:364–372. [PubMed: 16615920]

74. Mason CW, Swaan PW, Weiner CP. Identification of interactive gene networks: a novel approach in gene array profiling of myometrial events during guinea pig pregnancy. Am J Obstet Gynecol 2006;194:1513–1523. [PubMed: 16731067]
75. Buhimschi I, Christner R, Buhimschi C, Chaiworapongsa T, Romero R. Proteomic analysis of preterm parturition: a novel method of identifying the patient at risk for preterm delivery. Am.J.Obstet.Gynecol 2002;187:S55.
76. Romero R, Chaiworapongsa T, Gomez R, Kim YM, Edwin S, Bujold E, Yoon BH. Proteomic profiling of premature labor: a method to identify clinical biomarkers and mechanisms of disease. Am.J.Obstet.Gynecol 2003;189:S63.
77. Vuadens F, Benay C, Crettaz D, Gallot D, Sapin V, Schneider P, Bienvenut WV, Lemery D, Quadroni M, Dastugue B, et al. Identification of biologic markers of the premature rupture of fetal membranes: proteomic approach. Proteomics 2003;3:1521–1525. [PubMed: 12923777]
78. Monteoliva L, Albar JP. Differential proteomics: an overview of gel and non-gel based approaches. Brief.Funct.Genomic.Proteomic 2004;3:220–239. [PubMed: 15642186]
79. Gravett MG, Novy MJ, Rosenfeld RG, Reddy AP, Jacob T, Turner M, McCormack A, Lapidus JA, Hitti J, Eschenbach DA, et al. Diagnosis of intra-amniotic infection by proteomic profiling and identification of novel biomarkers. JAMA 2004;292:462–469. [PubMed: 15280344]
80. Ruetschi U, Rosen A, Karlsson G, Zetterberg H, Rymo L, Hagberg H, Jacobsson B. Proteomic analysis using protein chips to detect biomarkers in cervical and amniotic fluid in women with intra-amniotic inflammation. J.Proteome.Res 2005;4:2236–2242. [PubMed: 16335971]
81. Klein LL, Reisdorph N, Jonscher KR, Kushner EJ, Gibbs RS, McManaman JL. A Novel Method for Vaginal Proteomics in Preterm Labor. J.Soc.Gynecol.Investig 2006;13:144A.
82. Portilla D, Li S, Nagothu KK, Megyesi J, Kaissling B, Schnackenberg L, Safirstein RL, Beger RD. Metabolomic study of cisplatin-induced nephrotoxicity. Kidney Int 2006;69:2194–2204. [PubMed: 16672910]
83. Romero R, Gomez R, Nien JK, Yoon BH, Luo R, Beecher C, Mazor M. Metabolomics in premature labor: a novel approach to identify patients at risk for preterm delivery. Am.J.Obstet.Gynecol 2004;191:S2.
84. Izmirlian G. Application of the random forest classification algorithm to a SELDI-TOF proteomics study in the setting of a cancer prevention trial. Ann.N.Y.Acad.Sci 2004;1020:154–174. [PubMed: 15208191]
85. Jeffries NO. Performance of a genetic algorithm for mass spectrometry proteomics. BMC.Bioinformatics 2004;5:180. [PubMed: 15555060]
86. Levner I. Feature selection and nearest centroid classification for protein mass spectrometry. BMC.Bioinformatics 2005;6:68. [PubMed: 15788095]
87. Tan CS, Ploner A, Quandt A, Lehtio J, Pawitan Y. Finding regions of significance in SELDI measurements for identifying protein biomarkers. Bioinformatics 2006;22:1515–1523. [PubMed: 16567365]
88. Birkner MD, Hubbard AE, van der Laan MJ, Skibola CF, Hegedus CM, Smith MT. Issues of processing and multiple testing of SELDI-TOF MS proteomic data. Stat.Appl.Genet.Mol.Biol 2006;5:Article11.
89. Campbell G. Advances in statistical methodology for the evaluation of diagnostic and laboratory tests. Stat.Med 1994;13:499–508. [PubMed: 8023031]
90. Mossman D. Resampling techniques in the analysis of non-binormal ROC data. Med.Decis.Making 1995;15:358–366. [PubMed: 8544679]
91. Oppenheim, AV.; Schafer, RW. Digital signal processing. Prentice Hall; Englewood Cliffs, New Jersey: 1975.
92. Proakis, JG.; Manolakis, DG. Digital signal processing: Principles, Algorithms, and Applications. 3rd. Prentice Hall; Upper Saddle River, NJ: 1996.
93. Gonzalez, RC.; Wintz, P. Digital image processing. 2nd. Addison-Wesley; Reading, MA: 1987.
94. Kleijer WJ, De Bruijn HW, Leschot NJ. Amniotic fluid alpha-fetoprotein levels and the prenatal diagnosis of neural tube defects: a collaborative study of 2180 pregnancies in the Netherlands. Br J Obstet Gynaecol 1978;85:512–517. [PubMed: 79418]

95. Shields LE, Uhrich SB, Komarniski CA, Wener MH, Winter TC. Amniotic fluid alpha-fetoprotein determination at the time of genetic amniocentesis: has it outlived its usefulness? J Ultrasound Med 1996;15:735–739. [PubMed: 8908583]

96. Castagna A, Antonioli P, Astner H, Hamdan M, Righetti SC, Perego P, Zunino F, Righetti PG. A proteomic approach to cisplatin resistance in the cervix squamous cell carcinoma cell line A431. Proteomics 2004;4:3246–3267. [PubMed: 15378690]

97. Avasarala JR, Wall MR, Wolfe GM. A distinctive molecular signature of multiple sclerosis derived from MALDI-TOF/MS and serum proteomic pattern analysis: detection of three biomarkers. J Mol.Neurosci 2005;25:119–125. [PubMed: 15781972]

98. Tomosugi N, Kitagawa K, Takahashi N, Sugai S, Ishikawa I. Diagnostic potential of tear proteomic patterns in Sjogren's syndrome. J Proteome.Res 2005;4:820–825. [PubMed: 15952728]

99. Bast RC Jr. Badgwell D, Lu Z, Marquez R, Rosen D, Liu J, Baggerly KA, Atkinson EN, Skates S, Zhang Z, et al. New tumor markers: CA125 and beyond. Int.J Gynecol Cancer 2005;15(Suppl 3): 274–281. [PubMed: 16343244]

100. Hirtz C, Chevalier F, Centeno D, Rofidal V, Egea JC, Rossignol M, Sommerer N, Deville dP. MS characterization of multiple forms of alpha-amylase in human saliva. Proteomics 2005;5:4597–4607. [PubMed: 16294315]

101. Tabibiazar R, Wagner RA, Deng A, Tsao PS, Quertermous T. Proteomic profiles of serum inflammatory markers accurately predict atherosclerosis in mice. Physiol Genomics 2006;25:194–202. [PubMed: 16418319]

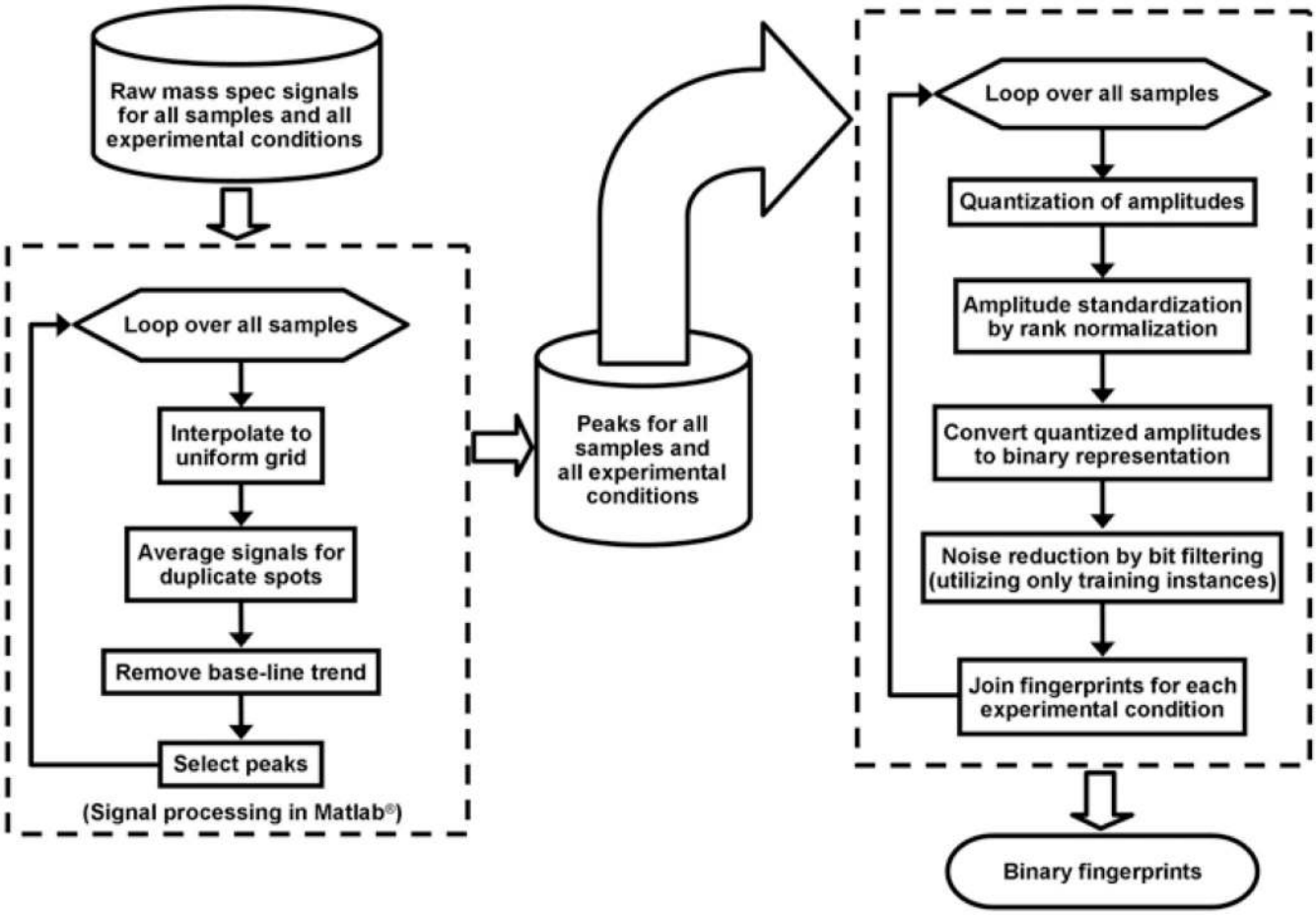

Figure 1.

Flowchart describing the elements involved in the transformation of raw mass spectrometry tracings to binary fingerprints necessary for pattern discovery. This flowchart consists of two major units denoted by dashed boxes. The box on the left side of this figure represents the processes conventionally referred to as "signal processing" in the engineering community. The box on the right side of the figure describes processes needed to transform signal data into a binary categorical description. Raw mass spectrometry files, stored as text files on computer disk, are first processed by computer programs written in the MATLAB® language. These processes are represented as rectangular boxes on the left side of this figure. Each mass spectrometry tracing is first interpolated to a uniform grid of m/z values. Next, signals corresponding to duplicate spots on the protein chip arrays are averaged. Then, the baseline trend for this averaged signal is removed. Finally, a set of peaks is obtained for each tracing. Thus, replacing the original signals by a set of selected features. As shown in the diagram, this sequence of processes is iterated over each tracing. These sets of peaks are stored in an intermediate file to be processed by operations on the right side of the diagram. The right side of this flow chart loops over all samples. First, for each sample, the sets of peak amplitudes are quantized. Next, the peak amplitudes are standardized by rank normalization. These quantized amplitudes are then converted into a binary representation. The next step of bit filtering is necessary in order to reduce noise. At this stage of processing, the data corresponding to each mass spectrometry tracing is represented as an individual binary sequence. Finally, binary sequences for each experimental condition for a given patient are concatenated, forming

a binary fingerprint accurately representing the data for a patient. These binary fingerprints form the input for pattern discovery.

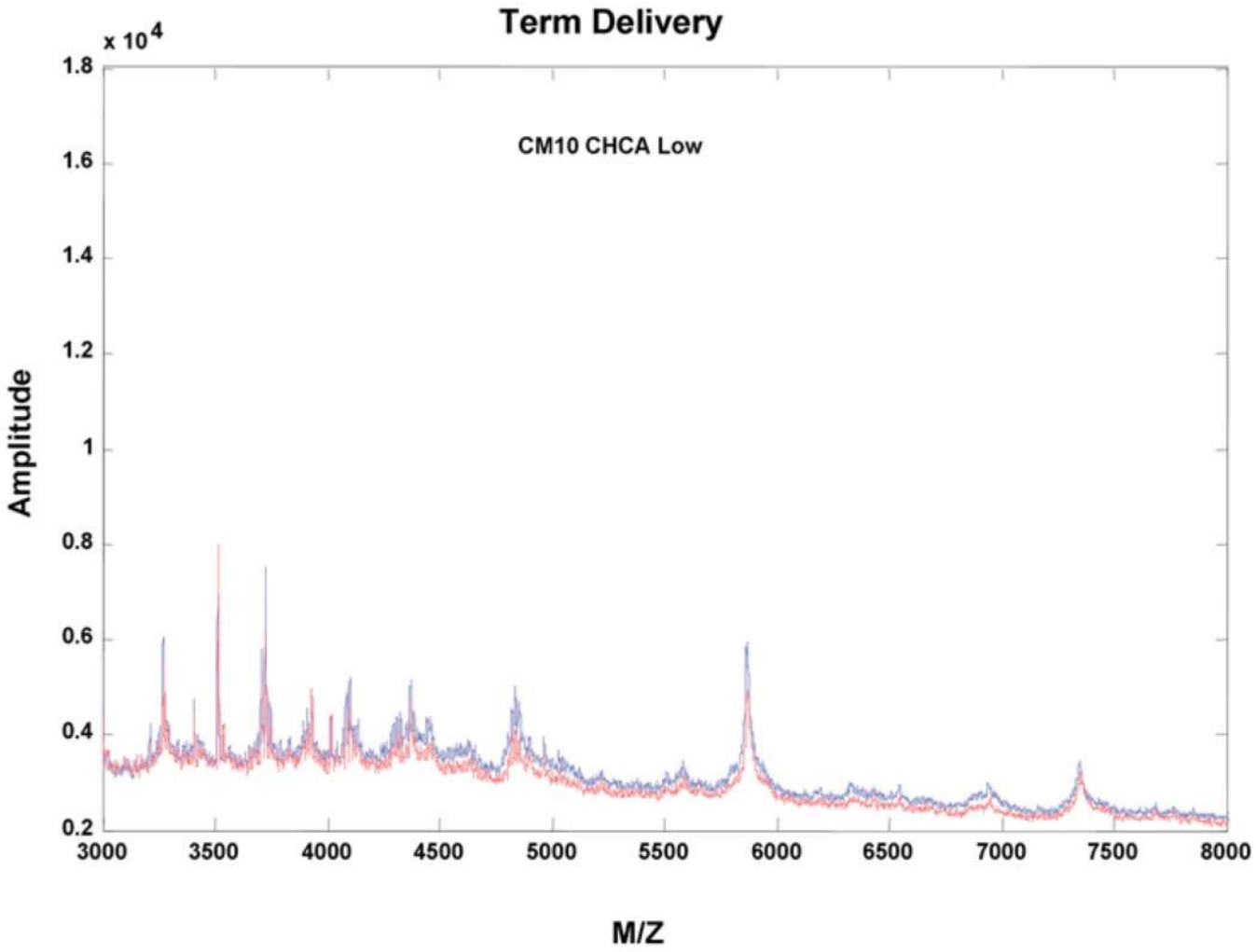

Figure 2.

Examples of raw mass spectrometry tracings of patients in the two clinical categories under study. Panel A describes the mass spectrometry tracing of the amniotic fluid of a patient with an episode of premature labor without inflammation who delivered at term. Panel B describes a similar tracing in a patient with premature labor with intra-amniotic infection/inflammation. Both tracings were generated using a CM10 (cationic chip), CHCA energy absorbing matrix at a lower laser intensity. Each panel displays two tracings, one for each of the duplicated spots (one tracing in red and one tracing in blue). Each sample of amniotic fluid was run in duplicate. Note first that the mass spectrometry profile of the same fluid is very similar, suggesting a high degree of reproducibility in both clinical categories (patients with preterm labor/delivery with intra-amniotic infection/inflammation and preterm labor without intra-amniotic infection/ inflammation who deliver at term). There are striking differences in the mass spectrometry profiles between the two clinical conditions. A large number of high-amplitude peaks are apparent in the tracing shown in panel B for the patient with preterm labor/delivery, with intra-amniotic infection/inflammation being absent in panel A. These high-amplitude peaks correspond to proteins present in patients with preterm labor/delivery with intra-amniotic infection/inflammation, while such proteins are either absent or in very low concentrations in patients with preterm labor without intra-amniotic infection/inflammation who deliver at term.

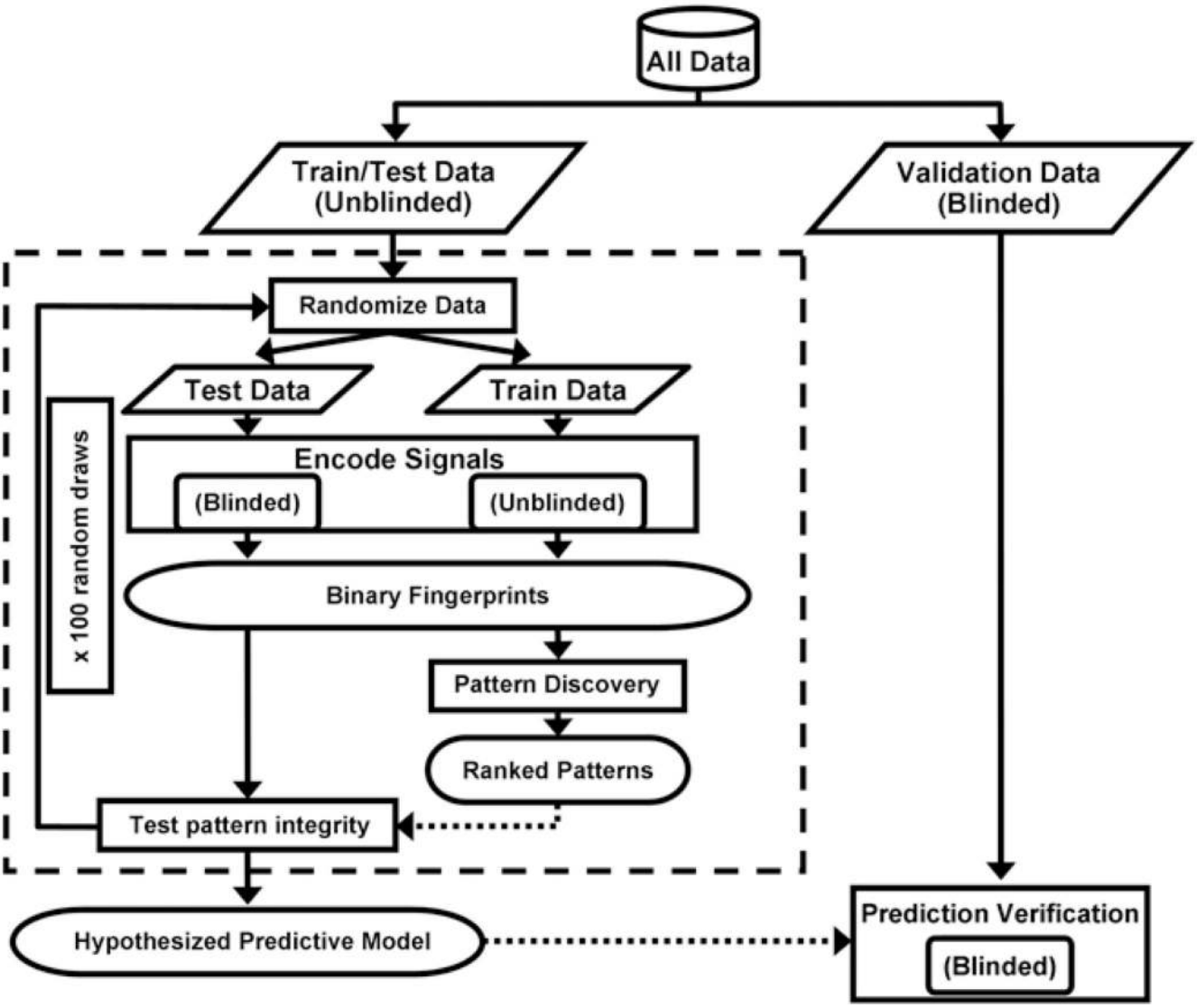

Figure 3.

Flowchart for the training/testing/validation. This diagram illustrates the cross-validation methodology employed in our analysis. First, data for all 119 patients were randomly divided into training/testing and validation samples. The training/testing sample consists of data for 88 patients: 44 with preterm labor/delivery with intra-amniotic infection/inflammation and 44 with preterm labor with term delivery. The validation set encompasses the remaining 31 patients: 16 with preterm labor/delivery with intra-amniotic infection/inflammation and 15 with preterm labor with term delivery. Data from the training/testing set follow the processing indicated on the left side of this diagram. The dashed box indicates the bootstrapping procedure of 100 repeated random draws in which 58 samples where selected for training data and 30 for testing data. Training and testing data sets were "balanced," with the training set containing 29 patients of each class and the testing set containing 15 of each class. Within one of these random draws, the classification of the training subset was available to the algorithms, while that of the test data were withheld (i.e., "blinded"). Encoding, as described in Figure 1, was carried out on the training and testing data resulting in binary fingerprints. Pattern discovery was performed on the training data to obtain sets of patterns for each of the two classes of data

(preterm labor/delivery with intra-amniotic infection/inflammation and preterm labor with term delivery). These patterns were ranked as to their relative information content with respect to the two clinical classes. The patterns from both classes were matched against each test instance in order to compute a score and classification for the test instance. Thus, the result of a single random draw was a set of classifications; one for each patient in the test sample for that draw. An entire run of 100 random draws resulted in a hypothesized predictive model, implicitly defined in terms of the encoding parameters for that run. After several runs were performed on the training/testing data, the one resulting in the best overall classification accuracy was selected for prediction of the validation data set, as indicated on the right side of this diagram.

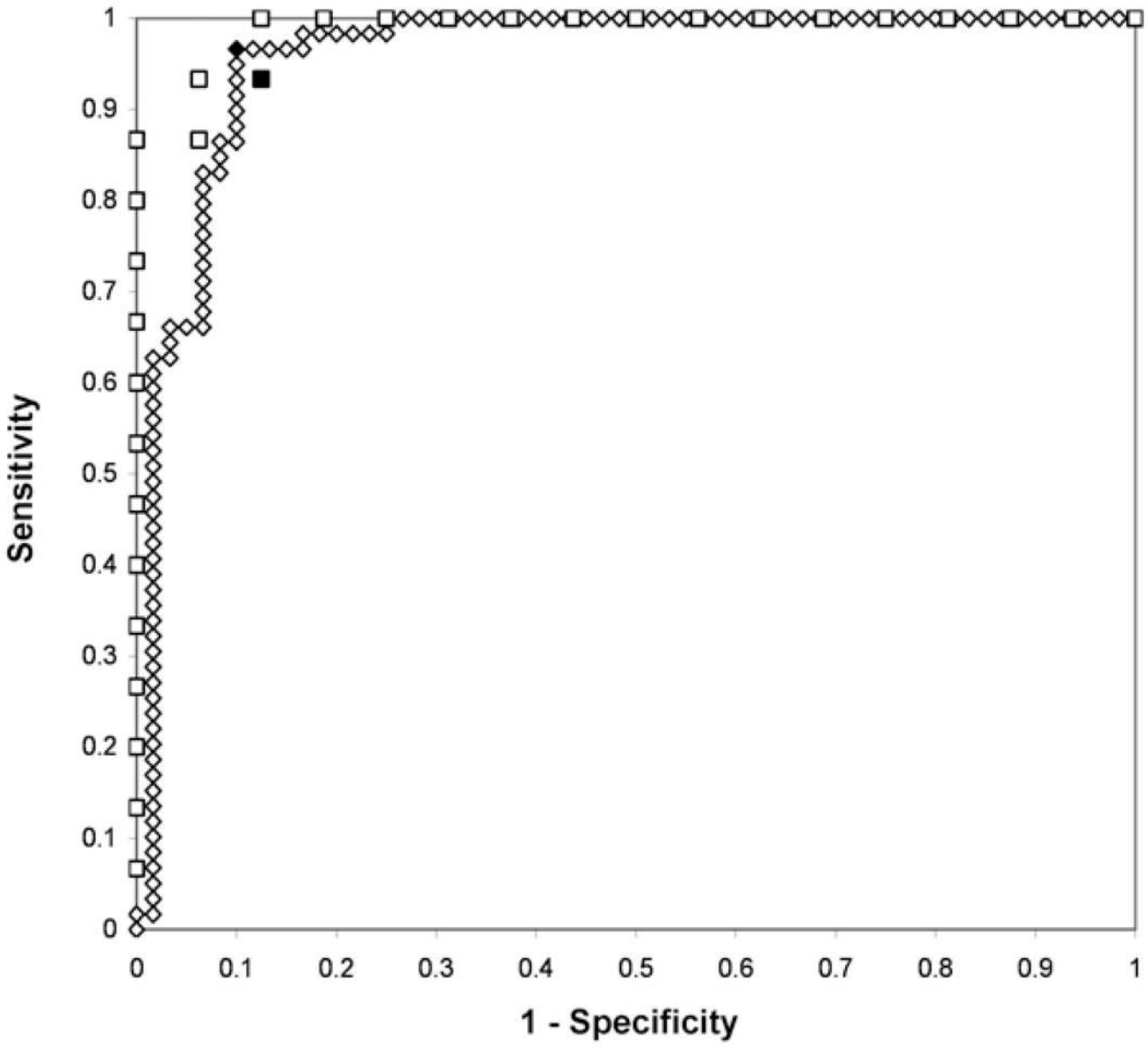

Figure 4.

ROC curves illustrating the relationship between sensitivity (vertical axis) and false-positive rate (1-specificity) in the horizontal axis. The ROC curve constructed with open diamonds is calculated using the average of over 100 random draws of the test scores received by each patient in the training/testing data set. The ROC curve constructed with squares is calculated from the scores obtained with the patients in the validation set. The filled symbols (squares and diamonds) represent the sensitivity/specificity point obtained by using 0 as the score cutoff for classification. Sensitivity and specificity are indicated in Table VI.

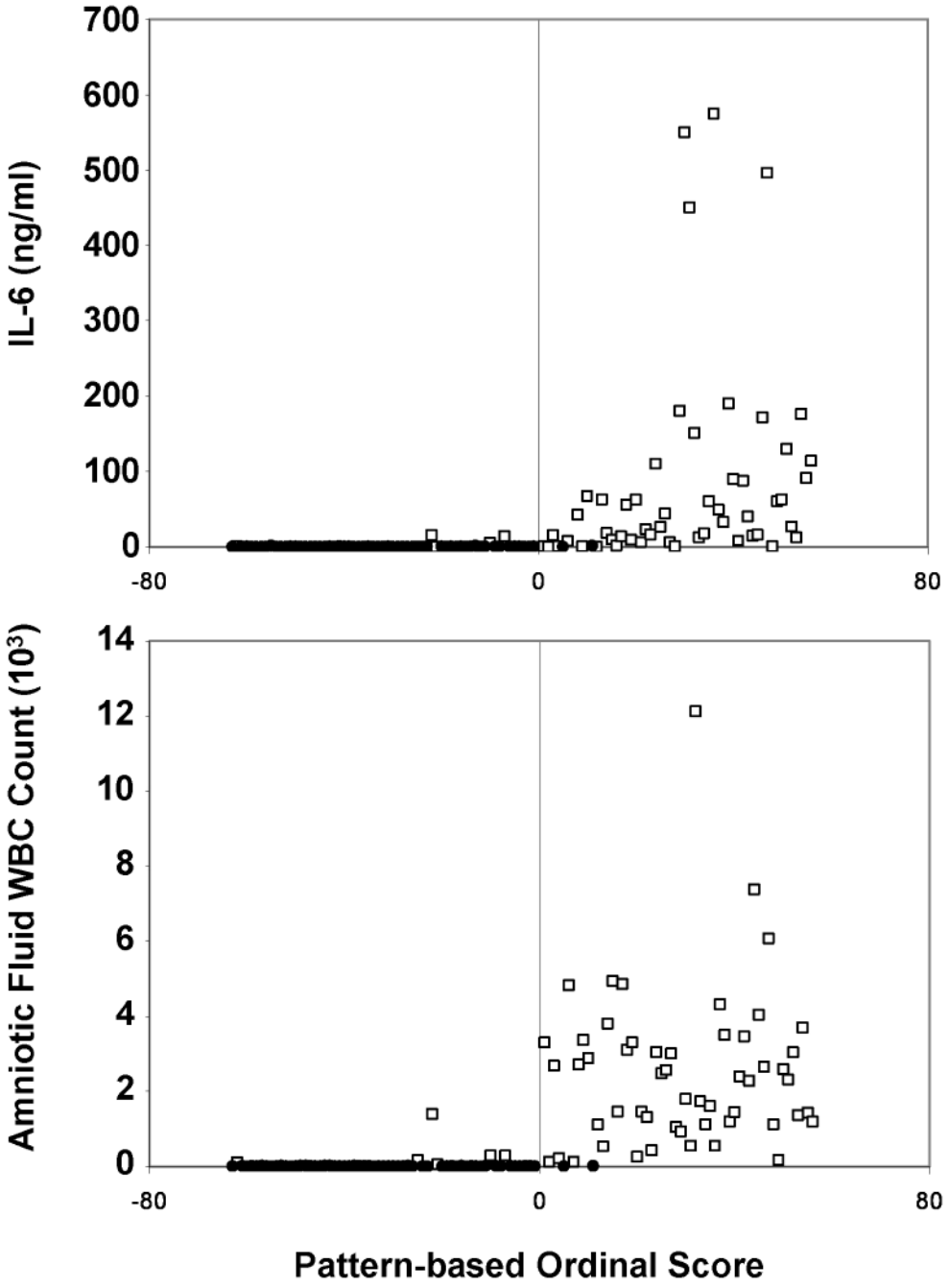

Figure 5.

Results of amniotic fluid analysis (amniotic fluid white blood cell count (WBC), IL-6 concentration) plotted versus pattern-based score, which is derived from proteomic analysis of amniotic fluid, as described in the Material and Methods section. The horizontal axis displays the rank of the pattern-based score. The lowest score is displayed on the left, and the highest score is displayed on the right. A negative value (to the left of 0) corresponds to patients whose classification, according to proteomic analysis of amniotic fluid, is predicted to be in the class of those who have preterm labor who subsequently deliver at term. A positive value (to the right of 0) corresponds to patients whose predicted classification is preterm labor/delivery with intra-amniotic infection/inflammation. The open boxes represent patients who have clinical

evidence of preterm labor/delivery with intra-amniotic infection/inflammation (this diagnosis was based on results of amniotic fluid analysis). The filled circles represent patients with an episode of preterm labor who delivered at term. There is a strong correlation between the ranked pattern score and the amniotic fluid WBC count (lower panel) and IL-6 concentration (upper panel). These results indicate that low scores (derived from proteomic analysis of amniotic fluid) are generally associated with both a low concentration of IL-6 in amniotic fluid and a low WBC count. Importantly, misclassified patients who are identified with empty boxes to the left of 0 had very low concentrations of IL-6 and/or amniotic fluid WBC count. This suggests that misclassification based on proteomic analysis occurred in patients with the mildest forms of intra-amniotic inflammation. Please note that this figure is based on all 119 patients, including the 88 in the training/testing data set and the 31 in the validation data set.

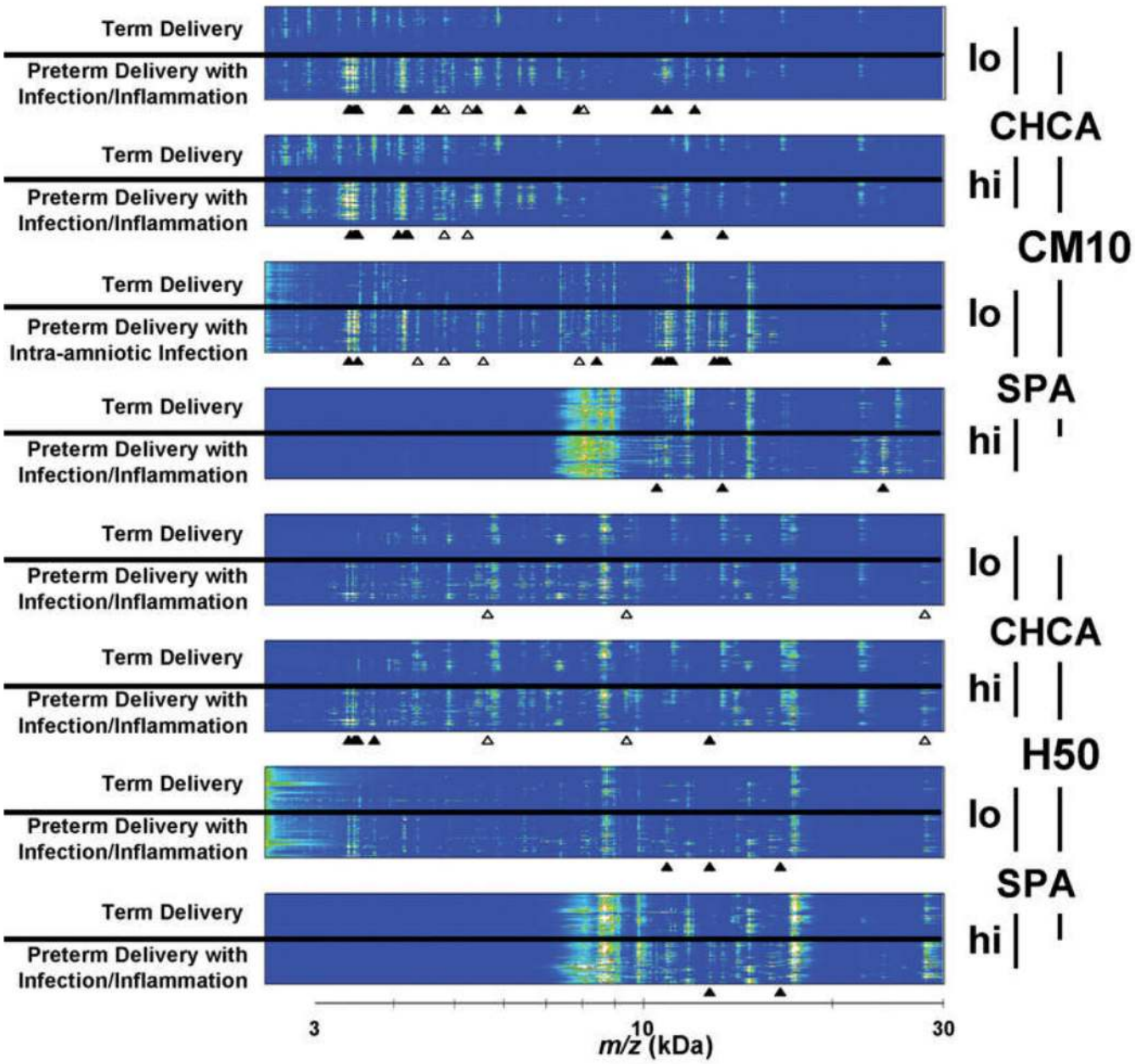

Figure 6.

Experimental data in heat graph format. Spectra have been detrended and resampled as described in the text. Colors indicate relative intensity of mass spectrometry signals (blue colors are low intensity, followed by greens, then reds and, finally, whites for maximum intensity). Each of the eight panels represents data collected with different experimental conditions which are indicated on the right side of the figure (lo/hi laser power, CHCA or SPA EAM, and H50 or CM10 chromatographic chip), and on each panel the preterm labor/delivery with intra-amniotic infection/inflammation patients are collected together below the preterm labor with term delivery patients. The m/z scale is logarithmic. The triangles underneath each panel indicate the location of features that are informative in discriminating the two patient groups. The filled triangles show stronger features identified in the first iteration of pattern discovery,

while the open triangles indicate weaker but still informative features identified in the second iteration.

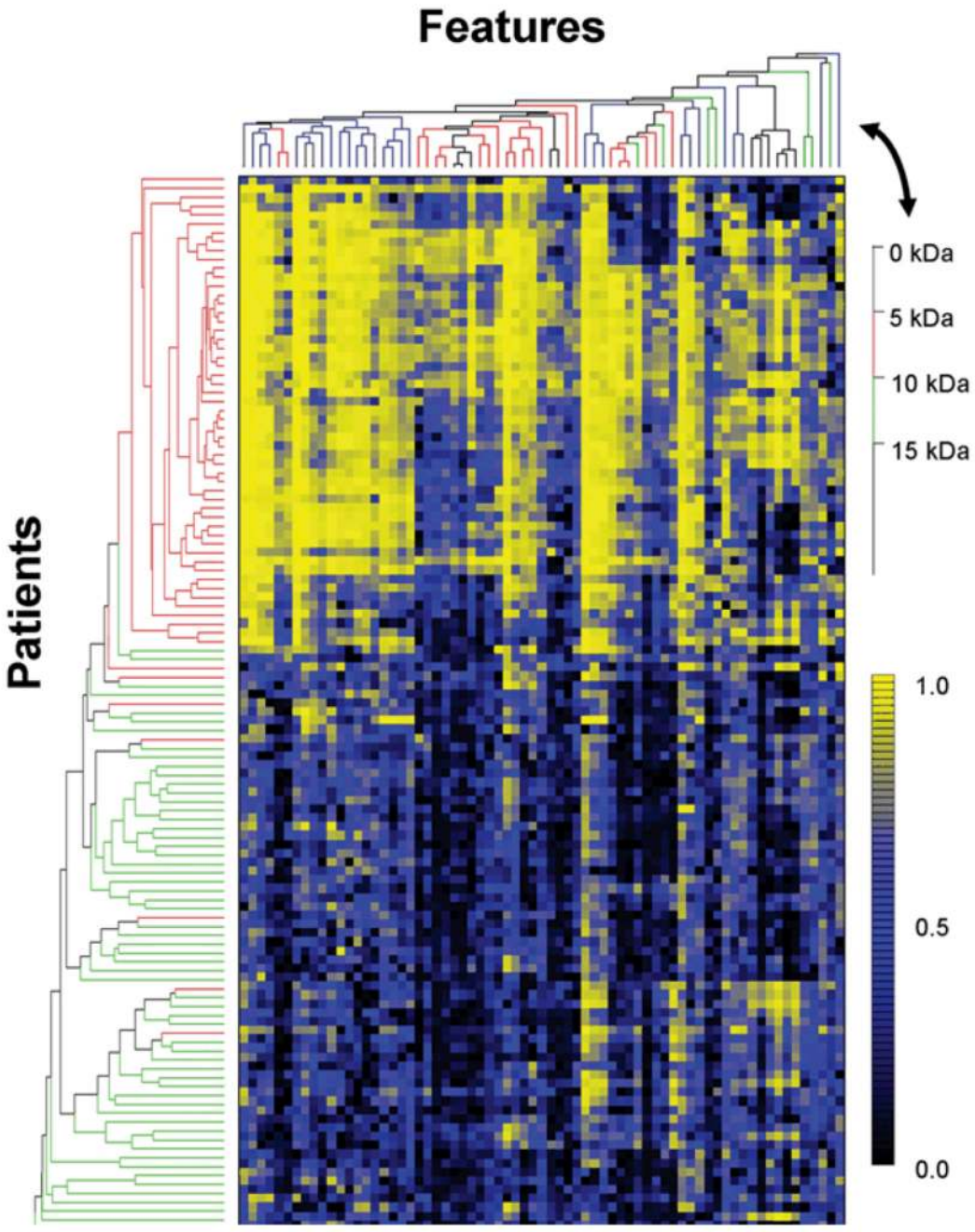

Figure 7.

Clustering of instances based on the "pattern" (i.e. the 69 features identified as described in the text corresponding to 39 distinct masses). The matrix has 119 rows (patients) by 69 columns. The spectral values corresponding to the binary features were retrieved from the spectra and rank normalized (as described in the text), such that the maximum value among the 119 × 9 values was 1.0 and the minimum value was 0.0. The color legend for the matrix is in the lower right. The dendrogram of patients (on the left side) is colored by clinical class (red = preterm labor/delivery with IAI, green = preterm labor with term delivery). The dendrogram of features (on the top) is colored by the *m/z* of the parent ion of the feature, with a color legend in the upper right.

Table I

Example of Differential Encoding.

Condition	Bit 1	Bit 2	Bit 3
Amplitude < T1	0	0	0
T1 ≤ Amplitude < T2	0	0	1
T2 ≤ Amplitude < T3	0	1	0
Amplitude ≥ T3	1	0	0

T1: low amplitude threshold.

T2: medium amplitude threshold.

T3: high amplitude threshold.

Bit 1: binary integer feature, which is set to 1 if the intensity is greater than the high amplitude threshold T3.

Bit 2: binary integer feature, which is set to 1 if the intensity is greater than the median amplitude threshold T2, but less than the high amplitude threshold of T3.

Bit 3: binary integer feature, which is set to 1 if the intensity is greater than the low amplitude threshold T1, but less than the median amplitude threshold of T2.

Table II

Example of Cumulative Encoding.

Condition	Bit 1	Bit 2	Bit 3
Amplitude < T1	0	0	0
T1 ≤ Amplitude < T2	0	0	1
T2 ≤ Amplitude < T3	0	1	1
Amplitude ≥ T3	1	1	1

T1: low amplitude threshold.

T2: medium amplitude threshold.

T3: high amplitude threshold.

Bit 1: binary integer feature, which is set to 1 if the intensity is greater than the high amplitude threshold T3.

Bit 2: binary integer feature, which is set to 1 if the intensity is greater than the median amplitude threshold T2, but less than the high amplitude threshold of T3.

Bit 3: binary integer feature, which is set to 1 if the intensity is greater than the low amplitude threshold T1, but less than the median amplitude threshold of T2.

Please note that this Table shows that bits remain set as the amplitude thresholds are exceeded.

Table III

Demographic and clinical characteristics of the study population (Training/testing sets)

	Term delivery (n=44)	Preterm delivery with IAI (n=44)	p
Maternal age (years)	21 (15-41)	25.5 (16-41)	NS
GA at amniocentesis (weeks)	29.9 (23-34)	28.1 (22-33)	NS
GA at delivery (weeks)	39 (37-42)	28.2 (22-34)	<0.001
Amniocentesis-to-delivery interval (days)	60 (34-130)	1 (0-11)	<0.001
Birthweight (grams)	3185 (2580-4560)	1240 (420-2600)	<0.001
AF WBC count (cells/mm^3)	3 (0-33)	470 (0-11000)	<0.001
AF glucose (mg/dl)	27 (0-107)	9 (0-58)	<0.001
AF IL-6 (pg/ml)	426.2 (45-1212)	76485 (2863-606000)	<0.001

Values are expressed as median (range).

IAI: intra-amniotic infection/inflammation; GA: gestational age; AF: amniotic fluid; WBC: white blood cell; IL: interleukin; NS: not significant.

Table IV

Demographic and clinical characteristics of the study population (Validation set)

	Term delivery (n=15)	Preterm delivery with IAI (n=16)	p
Maternal age (years)	23 (16-38)	29.5 (21-41)	NS
GA at amniocentesis (weeks)	31 (22-33)	27.9 (22-32)	NS
GA at delivery (weeks)	39.1 (37-40.7)	28 (23-33)	<0.001
Amniocentesis-to-delivery interval (days)	61 (33-130)	1.2 (0-7)	<0.001
Birthweight (grams)	3200 (2620-4500)	1189 (400-1940)	<0.001
AF WBC count (cells/mm^3)	0 (0-35)	655 (10-11500)	<0.001
AF glucose (mg/dl)	32 (17-83)	9 (0-60)	<0.001
AF IL-6 (pg/ml)	505.8 (164-1144.9)	114750 (6370-303700)	<0.001

Values are expressed as median (range).

IAI: intra-amniotic infection/inflammation; GA: gestational age; AF: amniotic fluid; WBC: white blood cell; IL: interleukin; NS: not significant.

Table V

Microbial and inflammatory status of the amniotic fluid in patients with preterm labor and intra-amniotic infection/inflammation who delivered preterm (Validation set)

Patient	AF Gram stain	AF culture	WBC count (cells/mm^3)	AF glucose (mg/dl)	AF IL-6 (pg/ml)
1	Gram (+) Cocci	Peptostreptococcus sp.	655	9	175300
2	Negative	Ureaplasma urealyticum		56	6370
3	Gram (+) Cocci	Fusobacterium sp., Ureaplasma urealyticum	2600	4	115500
4	Negative	Escherichia coli	310	9	69780
5	Gram (+) Cocci		11500	3	27340
6	Negative	Ureaplasma urealyticum, Staphylococcus epidermidis	1240	10	12600
7	Negative	Ureaplasma urealyticum	9920	3	303700
8	Negative	Ureaplasma urealyticum, Staphylococcus epidermidis	1250	8	129600
9	Negative	Ureaplasma urealyticum	362	10	190600
10	Negative		150	0	241100
11	Negative	Ureaplasma urealyticum	355	5	56100
12	Negative	Ureaplasma urealyticum	245	60	86630
13	Fungi	Candida sp.	280	1	14410
14	Fungi		800	18	114000
15	Negative	Capnocytophaga	10	14	164999
16	Negative		1120	28	155270

AF: amniotic fluid; WBC: white blood cell; IL: interleukin.

Table VI

Classification results for the Validation set.

	Predicted as preterm labor/delivery with IAI	Predicted as preterm labor with term delivery
Preterm labor/delivery with IAI	87.5 % (14/16)	12.5 % (2/16)
Preterm labor with term delivery	6.7 % (1/15)	93.3 % (14/15)

IAI: intra-amniotic infection/inflammation

Table VII

Biomarkers for patients with preterm labor/delivery with IAI

Avg *m/z*	Tier	Experimental Condition
3,380.6	1	cm10(chca), cm10(spa), h50(chca)
3,403.0	1	cm10(chca)
3,451.2	1	cm10(chca), h50(chca)
3,475.5	1	cm10(chca), h50(chca)
3,495.9	1	cm10(chca), cm10(spa), h50(chca)
3,716.9	1	h50(chca)
4,055.8	1	cm10(chca)
4,144.0	1	cm10(chca)
4,163.3	1	cm10(chca)
4,189.8	1	cm10(chca)
4,205.7	1	cm10(chca)
4,356.3	2	cm10(spa)
4,672.0	1	cm10(chca)
4,802.6	2	cm10(chca), cm10(spa)
5,232.4	2	cm10(chca)
5,430.2	1	cm10(chca) [z=2; 10,876.6 Da]
5,543.1	2	cm10(spa) [z=2; 11,094.6 Da]
5,632.8	2	h50(chca) [z=5; 28,086.5 Da]
6,354.5	1	cm10(chca)
7,869.6	1	cm10(chca)
7,891.2	2	cm10(spa)
8,020.7	2	cm10(chca)
8,409.3	1	cm10(spa)
9,383.4	2	h50(chca) [z=3; 28,086.5 Da]
10,483.6	1	cm10(chca), cm10(spa)
10,630.9	1	cm10(spa)
10,876.6	1	cm10(chca), cm10(spa), h50(spa)
10,993.6	1	cm10(spa)
11,094.6	1	cm10(spa)
12,055.2	1	cm10(chca)
12,737.1	1	h50(chca), h50(spa)
12,948.0	1	cm10(spa)
13,200.4	1	cm10(spa)
13,348.3	1	cm10(chca), cm10(spa)
13,526.3	1	cm10(spa)
16,512.9	1	h50(spa)
24,073.1	1	cm10(spa)
24,260.6	1	cm10(spa)
28,086.5	2	h50(chca)

The average m/z values in the first column describe the location of the biomarkers. Tier 1 and Tier 2 refer to the two stages of pattern discovery. Tier 1 features are more informative than those in Tier 2.